The Intra-Americas Sea: A Region of Challenges and Opportunities to Understand North American Climate Variability and Predictability

V. Misra[1,2,3], C. Wang[4], Y. Serra[5], K. Karnauskas[6], E. R. Martin[7], J. Sheinbaum[8], P. Chang[9,10,11], S. –K. Lee[4,12], B. Rosenheim[13], B. Kirtman[14], D. Enfield[4,12], E. D. Maloney[15], A. Kumar[16], G. Poveda[17], R. Fu[18], J. Jouanno[19], S. Berthet[19], A. Mishra[2], M. Bourassa[1,2], and J. Candela[8]

1 Department of Earth, Ocean and Atmospheric Science, Florida State University

2 Center for Ocean-Atmospheric Prediction Studies, Florida State University

3 Florida Climate Institute, Florida State University

4 Atlantic Oceanographic and Meteorological Laboratory, NOAA, Miami FL

5 University of Arizona

6 Woods Hole Oceanographic Institution

7 School of Meteorology, The University of Oklahoma

8 Oceanografia Fisica, CICESE

9 Texas A&M University, Department of Oceanography, College Station, TX, US, 77843

10 Texas A&M University, Department of Atmospheric Sciences, College Station, TX, US, 77843

11 Ocean University of China, Qingdao Collaborative Innovation Center of Marine Science and Technology, Qingdao, China, 266100

12 Cooperative Institute for Marine and Atmospheric Studies, University of Miami, Miami FL

13 College of Marine Science, University of South Florida

14 Rosenstiel School of Marine and Atmospheric Sciences, University of Miami

15 Department of Atmospheric Science, Colorado State University

16 Climate Prediction Center, National Centers for Environmental Prediction

17 Department of Geosciences and Environment, Universidad Nacional de Colombia, Sede Medellin, Colombia

18 Department of Geological Sciences, Jackson School of Geosciences, The University of Texas at Austin

19 Laboratoire d'Etudes en Geophysique et Oceanographie Spatiales

Abstract:
The Intra-Americas Seas (IAS), which includes the Gulf of Mexico and the Caribbean Sea is part of the largest warm water pool in the Western Hemisphere and is a primary moisture source for precipitation in the Americas. This IAS region is known to affect the North American climate variability across spatio-temporal scales as well as extreme weather events such as Atlantic tropical cyclones and southeast US tornadoes. The IAS also displays an active land-ocean-atmosphere interaction, with some of the largest river discharges producing extensive barrier layers which significantly affect the overlying atmospheric behavior. Most climate models display significant cold SST and dry rainfall bias over the IAS with a corresponding underestimation of their variability. In addition, significant biases in IAS surface and deep ocean currents, and poor representation of the atmospheric low-level jets in the region are also apparent in many climate models. Lack of observations in both the atmosphere and ocean in the IAS, which is one of the most poorly observed regions of the world, limits our ability to improve models. There are however emerging opportunities that could be leveraged to ameliorate some of these issues.

1 Introduction

The Intra-Americas Seas (IAS) comprising of the Gulf of Mexico (GoM) and the Caribbean Sea with its proximate location to North America and a seasonally appearing very warm SST (>28.5°C) in the boreal summer and fall seasons is recognized to be significant source of moisture that fuels the hydroclimatic variations of North America (Wang and Enfield 2001, 2003; Ruiz-Barradas and Nigam 2005; Mestas-Nunez et al. 2007). This body of warm water in the IAS with some parts of western tropical North Atlantic is a major part (over 80%) of the larger Western Hemisphere Warm Pool (WHWP; Wang and Enfield 2001; Fig. 1a), the second largest body of very warm water on Earth. A much smaller part of the WHWP resides in the northeast tropical Pacific west of Central America (also known as the Eastern Pacific Warm pool [EPWP]). The western tropical North Atlantic with the IAS is also collectively referred as the Atlantic Warm Pool (AWP). The WHWP is the second largest body of very warm water (≥28.5°C) on Earth and hosts the second largest diabatic heating center of the tropics during the boreal summer and fall seasons (Wang and Enfield 2001). The warm pool (≥28.5°C) appears initially in late boreal spring as EPWP followed by a warming of the AWP in boreal summer and fall seasons.

The IAS while geographically limited to the GoM and the Caribbean Sea is however dictated in its variations and teleconnections to the North American hydroclimate by symbiotic relation with overlying large-scale atmospheric circulation including the North Atlantic Subtropical High (NASH), the myriad atmospheric low level jets (LLJs; e.g. Caribbean, North American, Choco, Tehuantepec, Papagayo LLJs), complex cloud-radiation, and air-sea interactions. Additionally, ocean processes impacting the IAS region include the upper branch of the Atlantic Meridional Overturning Circulation (AMOC) that includes the Loop Current and the associated eddies in the GoM, prevalent subtropical cells, and the Caribbean current system with its ubiquitous mesoscale and sub-mesoscale eddies. Embedded within these defining features of the IAS are extreme events that are influenced by it like Atlantic tropical cyclones (TCs), tornadoes in the CONUS, large and intense meso-scale convective systems of the monsoons extending from central America to southwestern US (Maloney and Hartmann 2000a, b; Wang and Lee 2007; Wang et al. 2007, 2008a; Klotzbach 2014; Crosbie and Serra 2014; Serra et al. 2014).

The purpose of this paper is to highlight IAS variability that includes its surface and sub-surface oceanic and overlying atmospheric variability and its remote teleconnections to the climate of North America. This is followed by a discussion of the limitations of our current climate models and observational networks to effectively predict and monitor the observed IAS climate and its teleconnections over North America, respectively. We also present outstanding issues and emerging opportunities to improve climate predictability and monitoring of IAS variability spanning from intra-seasonal timescales to secular changes.

2 The IAS Variability

a) AWP Teleconnections

i) Sea Surface Temperature

The AWP defined by the 28.5°C surface isotherm (Fig. 1a) has a distinct seasonal cycle (Wang and Enfield 2001, 2003; Enfield and Lee 2005; Lee et al. 2007). It reaches a maximum in the area enclosed by 28.5°C in early September (Misra et al. 2014). The choice of the 28.5°C isotherm to define the AWP stems from its close correspondence with the variations in the IAS mixed layer depth (Wang and Enfield 2003), its notable impact on organized convection (Graham and Barnett 1987), and the display of the strongest interannual variations of the area enclosed by this isotherm in the IAS (Misra et al. 2013; Figs. 1b-d). The surface heat budget studies of the AWP indicate that the surface radiative fluxes dominate in the GoM while in the Caribbean Sea upwelling and advective cooling also play significant role in regulating the SST (Lee et al. 2007; Misra et al. 2013).

ii) Atmospheric circulation

The seasonal peak of the AWP-induced heating forces a Gill-type atmospheric response (to off equator forcing) as well as extratropical stationary waves (Fig. 2) that produces rainfall variability over the CONUS (Fig. 3a), while modulating the subtropical highs in the North Atlantic (Fig. 3b) and in the southeastern Pacific (not shown; cf Fig. 8 in Wang et al. 2010). AWP variations and their teleconnections to North American hydroclimate are also observed to be largely independent of the El Niño and the Southern Oscillation (ENSO) variations in the equatorial Pacific (Wang et al. 2006, 2008; Zhang and Wang 2012; Misra et al. 2013).

During the boreal summer season, the easterly trade winds advect moisture from the tropical North Atlantic (TNA) into the Caribbean Sea where the flow accelerates as the Caribbean low-level jet (CLLJ). To the first order the CLLJ is geostrophic (Wang 2007; Cook and Vizy 2010) and thus is controlled by the strong meridional pressure gradient established by the NASH and heating over northern South America (Fig. 1a; Amador and Magana 1999; Poveda and Mesa 1999; Wang 2007). Furthermore, Wang et al. (2008) and Rauscher et al. (2011) show that the magnitude of the SST anomaly in the Caribbean also influences the strength of the CLLJ. The CLLJ bifurcates as it transits the Caribbean Sea: one branch turning northward and forming the Great Plains LLJ (GPLLJ) while the other branch continues westward across Central America into the eastern North Pacific. Modeling and observational studies indicate that a large (small) AWP is associated with weakening (strengthening) of the summertime NASH and strengthening (weakening) of the summertime continental low over the NAM region (Fig. 3b; Wang et al. 2008a). The observational studies also confirm that in response to the pressure changes, a large (small) AWP weakens (strengthens) the southerly GPLLJ (e.g. Wang 2007), which results in reduced (enhanced) northward moisture transport from the GoM to the region east of the Rocky Mountains and thus decreases (increases) the moisture available for summer rainfall over the central United States (Wang et al. 2006; 2008; Ruiz-Barradas and Nigam 2006; Mestas-Nuñez et al. 2007).

iii) Precipitation

A strong (weak) easterly CLLJ associated with small (large) AWP area results in southerly (northerly) wind anomalies to the United States, which would transport more (less) moisture and consequently cause more (less) rain in the Great Plains region (Wang and Enfield 2003; Ruiz-Barradas and Nigam 2005; Wang 2007). Concomitantly, a strong CLLJ is associated with above normal rainfall over the Caribbean coast of Central America, including Nicaragua and Costa Rica, particularly during the boreal summer (May–September), through large-scale low-level convergence at the jet exit (Waylen et al. 1996; Magaña et al., 1999; Amador et al. 2000; Magaña and Caetano, 2005; Cook and Vizy 2010; Herrera et al. 2014). Such enhanced summertime convective activity on the upslope side of the terrain acts to deprive moisture to the Pacific coast of Central America and results in rainfall deficits there (Amador 1998; Cook and Vizy 2010; Martin and Schumacher 2011b).

The rainfall over the AWP alternates with the Amazon basin in South America as the seasonal heating source for the regional Hadley and Walker type circulations in the Western Hemisphere (Wang et al. 2006; 2010; Poveda et al. 2006). During the boreal summer/fall season, a strong regional Hadley-type circulation is established, with ascending motion over the AWP and subsidence over the southeastern tropical Pacific. A large (small) AWP during the boreal summer/fall results in a strengthening (weakening) of this regional Hadley-type circulation with enhanced descent (ascent) over the southeastern tropical Pacific (Wang et al. 2006, 2010, 2014; Lee et al. 2013b).

b) Secular change[1] in the IAS

[1] Secular change refers to the change in the variable in question with the sign of the change remaining the same throughout a long time period.

Among the challenges in interpreting observations of climate variability in the IAS region are the detection and attribution of low–frequency variability and long–term trends in SST. In particular, the IAS region is home to substantial internal multidecadal variability (Ting *et al.* 2011) that can mask forced long–term trends using instrumental records alone (Wang and Dong 2010) and often require historical hindcast model experiments to interpret (Ting *et al.* 2009). Moreover, future hydroclimate projections by state–of–the–art GCMs suggest that EPWP and most of the IAS region including the Caribbean islands, Central America, Mexico, and the southern United States should anticipate a robust and severe reduction in precipitation (Neelin *et al.* 2006; Meehl *et al.* 2007; Taylor *et al.* 2012; Maloney *et al.* 2014), which is thought to be critically dependent on the magnitude and spatial patterns of ocean warming (Schubert *et al.* 2009; Xie *et al.* 2010; Rauscher *et al.* 2011; Lee et al. 2011).

Future projections by the Coupled Model Intercomparison Project phase 5 (CMIP5) models predict that under the Representative Concentration Pathway (RCP8.5), GoM SST will warm in a spatially uniform fashion in the multi–model ensemble mean at a rate of 3–4°C century^{-1} by the end of the 21st century, and 2–3°C century^{-1} in the Caribbean Sea (IPCC AR5, WG1, Ch. 12, Fig. 12.11 [Collins *et al.* 2013]). The projected trends in these marginal seas approximately mirror those for the open Atlantic Ocean regions immediately to their east.

A comparison of four gridded instrumental datasets (see supplementary material [SM] S.1) agree on a broad warming across the western tropical Atlantic Ocean and the Caribbean Sea of ~0.4°C century^{-1} with the greatest warming found along the northern coast of South America in the southern Caribbean Sea (Fig. SF1). In a similar vein, the regional ocean model projections of Liu et al. (2015) suggest that there is a downward relaxation of isotherms along the coasts of Colombia and Venezuela to geostropically balance the weakening of the Caribbean Current, which further enhances the warming of the upper ocean. In stark contrast, the observed SST trends within the GoM are spatially heterogeneous and vary substantially from one product to another (Fig. SF1). Of particular relevance to recent and ongoing observational efforts is that SST changes in the GoM are highly divergent among the four data sets, varying by ~0.5°C relative to their 1951-1980 base periods. Published proxy reconstructions of water temperature corroborate the trends in the super ensemble of observations[2] (Fig. 4). The strongest proxy reconstruction trends are in the central Caribbean Sea (Fig. 4), where the super ensemble shows agreement with a positive trend. The weakest trends are in the GoM, but they are calculated from sediment cores with few points covering the 20th century (Richey et al, 2004; Richey et al., 2008). The record from the Cariaco Basin (off the north central coast of Venezuela; Black et al., 2008) is based on high time resolution through the 20th century, and it is the only proxy reconstruction in the basin that approaches the sign and magnitude of the trends in the super ensemble. The magnitude of these trends is based on species-specific calibrations that, in the case of the Caribbean Sea and GoM, seem to over-estimate long-term temperature change. It is important to note that records from Jamaica (Hasse-Schramm et al., 2003), Pedro Bank (central Caribbean, Haase-Schramm et al., 2003), and the Bahamas (Rosenheim et al., 2005) are from shallow subsurface records (28–67m). The general pattern of change in the instrumental SST

[2] See SM S.1 on further details of super ensemble of observations

products (smaller and/or less robust warming trends in the GoM than in the Caribbean Sea) is exactly opposite to the future trends projected by CMIP5 models.

However, it is important to point out that future projections by CMIP5 models may need to be downscaled or modeled at high resolution to better understand the regional response of the IAS, as the models seem to have significant ocean circulation bias in the IAS (Liu et al. 2102, 2015). Liu et al. (2015) downscaled the CMIP5 model simulations under historical and two future emission scenarios using an eddy-resolving regional ocean model. They reported that the simulated volume transport by the western boundary current system in the IAS, including the Caribbean, Yucatan and Loop Currents, was reduced by 20-25% during the 21st century, consistent with a similar rate of reduction in the AMOC. Their modeling analysis also showed that the projected reduction of the IAS western boundary current system was linked to reduced upwelling and enhanced warming along the western boundary. Over most of the GoM the downscaled model yields less warming than the low resolution IPCC models because of the latter’s inability to correctly resolve the volume transport through the Yucatan Channel and the Florida Straits.

c) The monsoons and the IAS

The IAS by its proximate location to the monsoons of the Americas serves as a bridge to unify the South American Monsoon (SAM) and North American Monsoon (NAM) systems. Observations have shown a negative correlation between boreal winter rainfall anomalies over the IAS region and those over the NAM and Southern Amazonia on interannual (Wang and Fu 2002) and multi-decadal time scales (Arias et al. 2015). On interannual time scales these relationships are linked by the reversal of the cross-equatorial flow over the Americas associated with ENSO (Arias et al. 2015). Misra and DiNapoli (2013) also find that the anomalous meridional migration of the ITCZ in the western Atlantic Ocean dictated by the intensity of the seasonal rainfall activity in the equatorial Amazon during boreal winter is negatively correlated with the upper ocean heat content (not shown) and surface temperature variability of the IAS in the subsequent seasons (Fig. 5). This teleconnection is established by the modulation of the atmospheric heat fluxes regulated by the overlying regional Hadley circulation, which gives rise to a robust negative correlation between austral summer rainfall over the equatorial Amazon and SST variability in the IAS during the subsequent boreal summer season.

On decadal time scales the negative correlation of rainfall between the NAM and the SAM is also related to the intensification of rainfall over the IAS region, causing an early retreat of the NAM and a late onset of the rainy season over southern Amazonia. These variations following Arias et al. (2012, 2015) seem to be a combined result of the westward shift of the NASH (a response to increased land-ocean contrast [Li et al. 201; Cook and Vizy 2010]) and the warm phase of the Atlantic Multidecadal Oscillation (AMO). The westward shift of the NASH enhances moisture transport from the IAS to the U.S. Great Plains, which in turn, weakens moisture transport to the NAM region (Arias et al 2012) and enhances the southerly cross-equatorial flow over South America and moisture export from southern Amaziona (Arias et al 2015). The warm phase of the AMO leads to warmer SST anomalies and stronger ITCZ over the TNA and northern South America, resulting in an equatorial contraction of the tropical meridional circulation over the American-Atlantic sector, stronger subsidence and moisture divergence over the NAM and southern Amazonia.

Previous studies on the sources of NAM moisture indicate that moisture at upper levels (above 700 hPa) originates to the east of the Sierra Madres Occidental and over the GoM, while low-level moisture of oceanic sources originates predominantly from the tropical Pacific Ocean and the Gulf of California (Schmitz and Mullen 1996; Adams and Comrie 1997). In addition to these oceanic sources, studies using a two-dimensional dynamic recycling model find that NAM terrestrial evapotranspiration accounts for approximately 40% of the total moisture sources to the NAM (Dominguez et al. 2006; Hu and Dominguez, 2015), similar to estimates of terrestrial sources for the May-July period based on moisture tracers in a GCM (Bosilovich 2003).

While the seasonal migration of the monsoon ridge is fundamental to the onset and demise of the NAM, monsoon precipitation is highly dependent upon intra-seasonal variability (ISV), especially in the southwestern United States at the northern edge of the monsoon. ISV in the IAS (see Serra et al. 2014 for a review) plays a particularly important role in supporting NAM rainfall events through gulf surges, or surges of moisture up the Gulf of California (e.g., Stensrud et al. 1997), and through IAS TC activity that recurves directly over the NAM region (Collins and Mason 2012; Ritchie et al. 2011; Corbosiero et al. 2009; Wood and Ritchie 2013). The link between tropical disturbances, gulf surges, the MJO, and NAM rainfall events has not been fully explored; however studies suggest that positive rainfall anomalies extend into the NAM region during the transition to the MJO westerly phase, when TC and easterly wave activity is also enhanced and shifted along the Mexican west coast (Lorenz and Hartmann 2006; Crosbie and Serra 2014; see SM [S.2])

The Mid-Summer Drought (MSD; Fig. 6) phenomenon characterized by a minimum rainfall that separates two peaks in rainfall across the Caribbean and Central America during boreal summer season has been associated with the westward expansion and intensification of the NASH and associated CLLJ variability resulting in moisture flux divergence (Hastenrath 1976, 1978; Granger 1985; Magana et al. 1999; Giannini et al. 2000; Mapes et al. 2005; Wang 2007; Wang and Lee 2007; Misra et al. 2014). As the NASH expands westward during the summer months precipitation is suppressed via large-scale subsidence and increased stability (Knaff, 1997; Mapes et al. 2005; Wang and Lee 2007; Kelly and Mapes 2011). In addition, the enhancement of the easterly trade winds in the southern Caribbean leads to greater evaporative cooling and lower SST which further suppresses summer convection (Muñoz et al. 2008, Xie 2006, Martin and Schumacher 2011b).

d) The ocean circulation in the IAS

The IAS is comprised of a very complex ocean circulation system from the smallest spatial scales (e.g. ubiquitous presence of mesoscale and sub-mesoscale eddies; see SM [S.3]) to hosting the upper branch of the AMOC (e.g. Caribbean current system, GoM loop current and the southern branch of the Gulf stream system). These ocean current systems that bring relatively warm and saline water from the equatorial Atlantic to the GoM are fundamental to the regulation of the SST in the IAS (Jayne and Maotzke 2002; Chang and Oey 2010; Liu et al. 2012; Misra et al. 2015). Owing primarily to shortcomings in long-term observational network of the IAS, substantial uncertainty exists regarding the magnitude of inter-annual flow variability within the channels (Yucatan, Old Bahama [OBC] and Northwest Providence [NWP] channels) that connect to the Florida Straits at 27° N (Rousset & Beal 2014; see SM [S.4]).

The southern Caribbean upwelling system significantly contributes to the mean SST distribution and its seasonal and interannual variability in the Caribbean Sea. The upwelling follows a semi-annual cycle resulting in surface manifestation of relatively cold SST, which peaks in December–March and July (Fig. 7) in response to semi-annual intensification of the along-shore CLLJ (Wang 2007; Wang and Lee 2007) and its associated changes in wind stress curl (Inoue et al. 2002; Andrade and Barton 2005; Cook and Vizy 2010). Jouanno and Sheinbaum (2013) also find that vertical turbulent mixing is important in regulating the surface cooling at the coast. The intense vertical mixing at the coast arises from vertical shear between the shallow and strong Caribbean Current and the subsurface Caribbean coastal undercurrent. This southern Caribbean upwelling region limits the southward extent of the AWP during its onset and peak phase (Lee et al. 2007) and modulates the meridional gradient of SST over the Venezuela and Colombia basins, with possible feedback to the trade winds (Chang and Oey, 2013). See SM (S.5) for further discussion on the rectification effect on the atmosphere from the cold SST's of this upwelling region.

It is also observed that a net freshwater gain (loss) in the TNA region coincides with the large (small) AWP regimes on interannual and multi-decadal timescales (Wang and Zhang 2013; Zhang and Wang 2012). They show that on these time scales, in association with large (small) AWP, warmer (colder) SSTs induce anomalous low-level convergence (divergence), which favors anomalous ascent (descent) that generates more (less) precipitation. Zhang et al. (2014) further confirm that this AWP induced freshwater flux plays a negative feedback role that acts to restore the AMOC from its anomalous state through basin-scale gyre circulation adjustments.

e) The IAS extreme events

A number of studies have shown that IAS variability modulates Atlantic TC activity (Fig. 8; e.g. Molinari et al. 1997; Maloney and Hartmann 2000a,b; Higgins and Shi 2001; Wang and Lee 2007, 2009; Wang et al. 2007, 2008a, 2011; Aiyyer and Molinari 2008; Jiang et al. 2012; Klotzbach 2014; Crosbie and Serra 2014). Calculated over a 34-year period (1979-2012), 90 named Atlantic TCs occurred in small AWP years versus 163 for large AWP years (Fig. 8). Wang and Lee (2007) argued that the observed relationship between AWP SST and Atlantic TC activity is a result of the AWP SST-forced changes of the vertical wind shear and moist static stability in the Atlantic TC Main Development Region (MDR).

Dynamically, the AWP-forced atmospheric circulation pattern is baroclinic within the tropical latitudes, with a large AWP producing a cyclone in the lower troposphere and an anticyclone in the upper troposphere, both situated on the northern flank of the AWP (Wang et al. 2008a; Fig. 2). This anomalous circulation structure reduces the lower tropospheric easterly flow and the upper tropospheric westerly flow in the MDR, thus reducing the vertical wind shear in a way that favors atmospheric convection (or TC development; Wang et al. 2007; 2008a). Similarly, the modulation of large-scale environmental factors including tropospheric humidity, vorticity, vertical shear, and SST by the MJO and other modes of ISV can also manifest in AWP-Atlantic TC and extreme rainfall teleconnections (Maloney and Hartmann 2000a; Camargo et al. 2009; Martin and Schumacher 2011a; Jiang et al. 2012). Furthermore, precursor disturbances for TCs in the form of easterly waves are also modulated on intraseasonal timescales in the IAS region (e.g. Maloney and Hartmann 2001; Crosbie and Serra 2014; Rydbeck et al. 2014). Thermodynamically, the AWP increases convective available potential energy (CAPE) that provides the fuel for moist convection and thus facilitates the formation and development of TCs (Wang et al. 2008). AWP-forced extra-tropical stationary Rossby waves influence the barotropic atmospheric flow over North America and the Atlantic in boreal summer (Lee et al., 2009), which then affects the steering flow of North Atlantic TCs (Wang et al., 2011; see SM [S.6]).

Boreal spring (April and May) is the primary season for tornadoes in the US. The convergence of dry upper level air from higher latitudes and low-level warm moist air from the GoM results in a conditionally unstable environment to the east of the Rockies with a raised CAPE that makes it conducive for tornadogenesis. Lee et al. (2013a) show that the April-May tornado outbreaks in the US are significantly correlated with moisture transport from the GoM (Fig. 9) and lower tropospheric vertical wind shear in the central and eastern US. Muñoz and Enfield (2011) find that the tornadic activity in lower Mississippi, Tennessee, and Ohio is particularly related to the interannual and decadal variability of the LLJs (Caribbean and North American) that dictate the moisture flux to the region (e.g., Maya express [Dirmeyer and Kinter 2009]).

f) The barrier layers of the IAS

The thick and persistent barrier layers or fresh water lens that form in the northwest tropical Atlantic Ocean is a result of the large volume of fresh water influx from some of the major continental rivers in northern South America (e.g., Orinoco and Amazon; Pailler et al., 1999). The barrier layers of the IAS are one of the most prominent structures in the world tropical and subtropical oceans (Mignot et al. 2007), which reflect the prevalence of the robust land-atmosphere-ocean coupling in the region. The mighty Amazon and Orinoco River systems together form the biggest river system in the world in terms of discharge (0.2 Sv). The Guyana current carries a significant portion of this water into the Caribbean Sea during boreal summer and fall (Hu et al., 1997), providing the largest term in the surface salinity balance of the region (Foltz and McPhaden, 2008; see SM S.7). Satellite and *in situ* observations confirm the occurrence of large interannual anomalies in the spatial extent of the riverine barrier layer over the western TNA and eastern Caribbean (Johns et al. 2014; Fig. SF8).

Because of the barrier layer role in trapping heat within the upper ocean layer and reducing surface cooling, the barrier layer in the northwestern tropical Atlantic has the potential to affect Atlantic TC activity (Ffield 2007; Vizy and Cook 2010, Balaguru et al. 2012). When TCs pass over barrier layers, the reduced efficacy of vertical mixing in these highly stratified layers leads to reduced SST cooling, which then impacts TC evolution by maintaining strong air–sea fluxes. In the northwestern tropical Atlantic, Balaguru et al (2012) reported that the mean rate of increase of intensity of Atlantic TCs increases from 0.48 ms^{-1} over a 36-hour period in non-barrier layer regions to 0.98 ms^{-1} over the same time period in barrier layer regions.

3 The limitations of numerical models simulating and predicting IAS climate

The surface temperature of the IAS and its variability are grossly underestimated by a majority of the CMIP models that participated in the IPCC AR4 and AR5 especially in the boreal summer and fall seasons (Fig. 10; Misra et al. 2009; Kozar and Misra 2012; Liu et al. 2012, 2013; Ryu and Hayhoe 2013). A majority of the CMIP5 models underestimate the area of the AWP in their 20th century simulation (Fig. 10). Surface heat budgets computed over the IAS reveal that the radiative fluxes of downwelling shortwave and longwave radiation dominate the maintenance of the AWP (Misra et al. 2013). However, the important and subtle role for air-sea turbulent fluxes in the variability of the AWP and its interplay with the variability of the overlying low-level easterlies, which is related to the strength and position of the NASH, cannot be overemphasized (Misra et al. 2009). Liu et al. (2012) and Misra et al. (2013) find that a majority of current global circulation models (GCMs) and reanalysis products of the ocean and the atmosphere produce a qualitatively consistent surface heat budget in the IAS. However, when compared to reanalysis, GCMs have a tendency to underestimate latent heat flux and downwelling shortwave flux, and overestimate sensible heat flux. Liu et al. (2012) also indicate that the upper ocean heat budget in the GoM is a complex balance of contrasting warming influence of upper ocean heat transports (e.g. Loop Current) and cooling influence of the net surface heat flux. With significant GCM biases prevalent in surface fluxes and ocean circulation over the region (Liu et al. 2015), it is not surprising to note such large SST errors over the IAS in GCMs (Fig. 11). In addition, Xu et al. (2014) found that the persistent warm bias over southeastern tropical Atlantic across generations of climate models (Fig. 11; e.g. Richter and Xie, 2008; Richter et al. 2014) can remotely force a significant cold SST bias and dry precipitation bias in the IAS region (cf. their Fig. 18; Xu et al. 2014).

The IAS region is also characterized by significant deficiencies in the simulation of convection and related processes. For example, ISV in the east Pacific and Caribbean is poorly simulated in amplitude and spatial structure in climate models (Jiang et al. 2013), with poor performing models also tending to have common mean state biases in winds and other fields. Model ISV in the IAS region can be improved by suppressing convection through enhanced moisture sensitivity or other means, although often the quality of the mean state degrades when such modifications are not done with care (e.g. Kim et al. 2011; Maloney et al. 2014a), suggesting that such changes can improve ISV for the wrong reasons (e.g. Maloney et al. 2014a; Hannah and Maloney 2014). Martin and Schumacher (2012) and Ryu and Hayhoe (2013) showed that the cold SST bias in the IAS further exacerbates the dry rainfall bias over the Caribbean and central America across CMIP3 coupled historical simulations. In recent CMIP5 historical simulations, large precipitation and SST biases across the Caribbean are still evident in both coupled (historical) and uncoupled (AMIP) simulations (see SM [S.8]; Sheffield et al. 2013). Furthermore, the timing of NAM precipitation also exhibits substantial biases, with models generally producing too little precipitation in the NAM region in early and mid boreal summer, and excessive precipitation late in the monsoon period (Liang et al. 2008; Sheffield et al. 2014a), associated with difficulty in ending the monsoon (Geil et al. 2013).

The recent effort to make seasonal predictions from multiple models like the North American Multi-Model Ensemble project (NMME; Kirtman et al. 2014) routinely available allows us to assess skill of predicting SSTs over the AWP, and land-surface (e.g. precipitation, surface temperature) anomalies over the surrounding areas. Misra and Li (2014) find that the seasonal predictability of the AWP in the NMME models is promising compared to earlier generation GCMs (Misra et al. 2009), but also displays notable limitations. For example, NMME mean forecasts indicate that skill in predicting seasonal mean SSTs in the AWP is much less than the skill in predicting SST variability in the equatorial eastern Pacific associated with ENSO (Niño3.4 region; Fig. 12). Anomaly correlations averaged over the AWP region are in the range of 0.5 – 0.6, much less compared to those over the eastern equatorial Pacific (Niño3.4 region). Prediction of terrestrial climate anomalies around the IAS relies on skillful prediction of IAS SSTs, and hence seasonal prediction over land areas cannot be improved until skill in predicting SST is improved. An assessment of the corresponding JJA seasonal mean precipitation anomalies confirms this (Fig. 13) in which prediction skill (anomaly correlation of the ensemble mean) generally does not exceed 0.3. See SM (S.10) for comparison of this skill with the boreal winter season.

4 The observing network in the IAS

A gradually and significantly degrading observational network for the atmosphere and ocean in the IAS region also exacerbates the modeling challenges described in the previous section. For example, the radiosonde network in the region is quite sparse (Fig.

SF10; SM [S.9]) and is currently unable to sample the core of the CLLJ. In addition, for a region that displays a highly heterogeneous distribution of rainfall, the rain gauge network is highly inadequate (Fig. SF11). The complex spatial structure of rainfall in the IAS (with topographic, island, and LLJ effects) raises a challenge for observing and monitoring the climate of the region. For example, Figs. 6a and b show rainfall measurements from the satellite based Tropical Rainfall Measuring Mission (TRMM) and merged satellite and in-situ Global Precipitation Climatology Project (GPCP) data, respectively, and differences between the products are evident in both the location and magnitude of rainfall features across the region, which is largely a reflection of the differences in spatio-temporal resolution of the two datasets. Using TRMM precipitation radar data, Sobel et al. (2011) show that rainfall enhancement relative to the surrounding oceanic region is more significant over larger (greater than 315 km^2) islands than smaller islands in the Caribbean and that smaller islands have a negligible or even negative change in rainfall intensity and frequency relative to surrounding oceans. However, while high-resolution satellite data such as TRMM and the newly launched Global Precipitation Measurement (GPM) satellites can provide useful information, the 0.25° TRMM resolution (~28km) provides fewer than 3 measurements for most of the smaller islands in the Lesser Antilles. For example, the island of Dominica (approximately 25km wide and 50 km long) has large zonal variations in rainfall intensity and frequency as measured during the DOMEX (Dominica Experiment) field campaign that are not captured by current satellite measurements of rainfall (Smith et al. 2012, Minder et al. 2013).

In-situ ocean observational networks in the IAS have also diminished considerably over time. ARGO floats, which have the operating depth of about 2000m cannot pass the Lesser Antilles to reach the Caribbean Sea. As a result, the IAS is currently one of the most mostly poorly observed oceans at depth (Fig. SF12). This poor observational network leaves some basic issues unresolved including characteristics of the seasonal cycle of the oceanic variables in the IAS and its relation to the Loop Current and eddy shedding dynamics, and the different pathways of the flow that can impact the salt, temperature and fresh water transport by the AMOC through the western boundary. As mentioned earlier, there is significant disparity in the diagnosis of the observed long-term variations of SST in the IAS.

One promising area for alleviating the lack of ocean profile data in the IAS is the deployment of ocean gliders that can sample temperature, salinity and other variables at depths up to 1000 meters. At present there are an average of 10 gliders operating in the GoM at any given time but fewer than half of them transmit publicly available data through the global telecommunication system (GTS). Only two gliders operate in the Caribbean north and south of Puerto Rico, the basis of a pilot project designed to assess the potential of gliders for predicting the intensification of hurricanes. However the project sunsets in 2015 and no other glider sampling is projected for the Caribbean. Glider sampling has its limitations and can’t entirely satisfy the need for subsurface ocean data. But because research vessels are expensive and ARGO floats can’t be navigated away from grounding depths in a confined marginal sea, more glider-based research is clearly needed, especially in the Caribbean.

5 Discussion and Conclusions

i) Outstanding issues

A growing body of literature on IAS climate has revealed that IAS is a primordial soup of a spectrum of important scales of variations that has to be viewed not in isolation but as part of the complex surrounding land, local and remote oceans and atmosphere. The continued underperformance of the global models over the IAS through several generations of model development is of grave concern. The IAS provides an ideal test bed in the proximate location of North America:

- To examine the role of scale interactions in the manifestation of its important scales of variations; the synergy of the IAS mean state and variations with the atmospheric LLJ's and the mesoscale eddies in the ocean has to be more clearly understood.
- To understand the mechanisms of a seasonally persistent warm pool and the stratification of the upper ocean vis-à-vis continental monsoon dynamics and convection in the barrier layer formation; similarly the role of ocean dynamics, air-sea fluxes, and cloud radiative feedbacks has to be more carefully studied in the context of the AWP.
- The delineate source of variability from natural and anthropogenic influence in a region like the IAS is very important as it displays robust manifestation of the AMO and hosts the upper limb of the AMOC.
- The role of dust and Saharan Air Layer (SAL) in the IAS climate variations and their influence on the genesis of TC in the western Atlantic have to be further quantified.
- The uncertainty in the diagnosis of long-term changes in the surface temperature of the IAS needs to be reconciled while equally importantly quantification of

changes to upper ocean stratification is necessary to understand the observed long-term changes in upper ocean tropical cyclone activity

- Climate projections for the IAS have to be understood more holistically than in isolation especially when it is being recognized that land hydrology has an important role to play both via river discharges into the IAS as well as through atmospheric response to latent heat release.
- In the absence of far less than ideal observing systems, reconstruction of the history of IAS climate especially to decipher important variations of features like LLJ's, mid-summer drought, tropical cyclones, mesoscale convective systems is dependent on developing robust reanalysis at significantly high resolution that take in to account the land hydrology-ocean-atmosphere interactions.

ii) Emerging opportunities

Coordinating with ongoing projects, partnering with local organizations in the region, and leveraging technological advances could significantly ameliorate the observational gaps in the IAS and its adjacent nations. For example, in response to the need to monitor both short and long term natural hazards throughout the Caribbean and Mexico, the National Science Foundation (NSF) has funded two GPS-based atmospheric sounding initiatives: The Continuously Operating Caribbean Observation Network (COCONet) (Braun et al. 2012) and the Trans-boundary, Land and Atmosphere Long-term Observational and Collaborative Network (TLALOCNet) in Mexico. Mexican partners, including the National Autonomous University of Mexico (UNAM) will also add to this network (see SM S.11). Data products from these networks include estimates of column integrated tropospheric water vapor; surface meteorological variables including wind speed and direction, air temperature, humidity and precipitation; time series of daily positions and component velocities for each station (used to quantify tectonic changes in the region); and high-rate low-latency data from a subset of stations. Similarly, new techniques like Global Positioning System (GPS) Radio Occultation (RO) measurements can provide relatively accurate atmospheric sounding data with high vertical resolution especially above the atmospheric boundary layer (Anthes et al. 2008) that could supplement the sparse upper air network in the region.

Several important measuring and modeling projects for the GoM are currently in progress or are about to be financed either by the oil industry and/or government agencies from different countries (e.g. the Gulf of Mexico Research Institute). A coordinated approach to achieve some basic common goals among these projects could help sustain a multinational long-term observing and monitoring program at least for the GoM. In addition, new technologies including underwater gliders appear to be particularly ideal for setting up a relatively low cost long-term observing program for the IAS in which cross-sections across the Caribbean Current or in the GoM could be regularly sampled. Choosing some of these sections to coincide with satellite-altimetry tracks would provide invaluable information for calibration of altimetry against observed stratification and heat content. Glider observations seem especially well suited for studies of hurricane intensification, which could be supplemented with greater coverage by surface drifters and IRIDIUM-controlled ARGO floats. A pilot underwater glider project for the Caribbean Sea has already started since 2014 (http://www.aoml.noaa.gov/phod/goos/gliders). Coordinated intensive field observations can also be planned to provide high temporal and spatial resolution atmospheric and oceanic observations in limited regions to better understand local and regional physical process and to provide high quality datasets for improving models. High resolution modeling studies may also provide a bridge to improving global model physical parameterizations, if coordinated with such field programs. The fundamental challenge for future IAS research is to create sustainable funding to maintain these observational systems (e.g., gliders and GPS networks). There are also ongoing efforts to rescue historical meteorological data in the Caribbean through the Caribbean Agro-Meteorological initiative (http://www.cimh.edu.bb/cami/). Likewise there are capacity building measures by Caribbean Institute for Meteorology and Hydrology and other such regional institutions which raise our hopes to promote better observational platforms in the region.

Another of the current grand challenges in seasonal-to-interannual prediction is rainfall during the warm season over North America, which is a difficult problem because much of the rainfall is associated with relatively small-scale structures (e.g., thunderstorms and mesoscale convective complexes) that are not adequately resolved by the current generation of seasonal-to-interannual prediction systems. As a consequence, large systematic errors occur in the predicted rainfall anomalies that seriously limit forecast quality. Fundamental predictability issues also exist, namely that remote forcing from remote climate variability (e.g. ENSO) is relatively weak and the rainfall signal-to-noise ratio over North America is comparatively small. Nevertheless, our current understanding indicates that current prediction systems are underperforming, even with the limited predictability (see SM [S.10]).

The IAS climate processes outlined in this paper provide opportunities to improve local and remote North American hydroclimate prediction across temporal scales. An opportunity also exists to provide a more holistic picture of Western Hemisphere climate and its prediction by bridging tropical South American climate variability with that of the IAS. Moving forward, the modeling and observational challenges of IAS have to be overcome for improved climate monitoring and prediction of North America.

Acknowledgements

We acknowledge the help of graduate student Michael Kozar of FSU in preparing Fig. 8. We also thank Kevin O'Brien of NOAA for generating Fig. SF12. We thank the three anonymous reviewers who greatly helped in improving this manuscript from its earlier version with their thoughtful suggestions. We also acknowledge the support of NSF, NASA, NOAA, CISCE. Chunzai Wang, Sang-Ki Lee and David Enfield acknowledge the support of the base funding to NOAA/AOML. We also acknowledge data resourced from the NOAA/OAR/ESRL PSD, Boulder, Colorado, USA, from their Web site at http://www.esrl.noaa.gov/psd/, UCAR from their website http://dss.ucar.edu

References

Adams, D. K., and A. C. Comrie, 1997: The North American Monsoon. Bull. Amer. Meteor. Soc, 78, 2197–2213.

Amador, J. A., 1998: climatic feature of the tropical Americas: The trade wind easterly jet. Top. Meteor. Oceanogr. 5, 91–102.

Amador, J. A., and V. O. Magaña, 1999: Dynamics of the low level jet over the Caribbean, in 23rd Conference on Hurricanes and Tropical Meteorology, pp. 868–869, Am. Meteorol. Soc., Dallas, Texas.

Amador, J., Magaña, V., and Pérez, J., 2000: The low level jet and convective activity in the Caribbean. In Preprints 24th Conf. in Hurricanes and Tropical Meteorology, Fort Lauderdale, FL, AMS, pp. 114–115.

Andrade, C. A., and E. D. Barton, 2005: The Guajira upwelling system. Cont. Shelf Res., 25, 1003–1022.

Anthes, R. A., Y. H. Kuo, D. P. Baumhefner, R. P. Erico, and T. W. Bettge, 1985: Predictability of mesoscale atmospheric motions. *Advances in Geophysics,* Vol. 28B, Academic Press, 159–202, doi:10.1016/S0065-2687(08)60188-0.

Aiyyer, A. and J. Molinari, 2008: MJO and Tropical Cyclogenesis in the Gulf of Mexico and Eastern Pacific: Case Study and Idealized Numerical Modeling. J. Atmos. Sci., 65, 2691–2704.

Athie, G., Sheinbaum, J., Ochoa, J., Candela J., Leben, R. Interannual variability of the flow at Yucatan Channel, submitted, Geophysical research letters, 2014.

Arias, P. A., R. Fu, C.S. Vera, and M. Rojas, 2015: A correlated shortening of the North and South American monsoon seasons in the past few decades. *Climate Dynamics*, 10.1007/s00382-015-2533-1.

Arias, P.A., R. Fu, and K. C. Mo, 2012: Decadal variation of rainfall seasonality in the North American Monsoon region and its potential causes. J. Clim., 25, 4258-4274.

Black, D.E., Abahazi, M.A., Thunell, R.C., Kaplan, A., Tappa, E.J., Peterson, L.C., 2007. An 8-century tropical Atlantic SST record from the Cariaco Basin: Baseline variability, twentieth-century warming, and Atlantic hurricane frequency. Paleoceanography 22, 10.

Bosart, L. F., G. J. Hakim, K. R. Tyle, M. A. Bedrick, M. J. Dickinson, and D. M. Schultz, 1996: Large-scale antecedent conditions associated with the 12–14 March 1993 cyclone (‘‘Superstorm ’93’’) over eastern North America. Mon. Wea. Rev., 124, 1865–1891.

Bosilovich, M. G., 2003: Numerical simulation of the large-scale North American monsoon water sources. Journal of Geophysical Research Atmosphere, 108, 8614, doi:10.1029/2002JD003095.

Braun, J., and Coauthors, 2012: Focused Study of Interweaving Hazards Across the Caribbean. Eos, Trans. Amer. Geophys. Union, 93, 89–90.

Breugem W.-P., P. Chang, C. J. Jang, J. Mignot and W. Hazeleger, 2008: Barrier layers and tropical Atlantic SST biases in coupled GCMs, Tellus A, 60, 885–897, DOI: 10.1111/j.1600-0870.2008.00343.x.

Camargo, S. J., M. C. Wheeler, and A. H. Sobel, 2009: Diagnosis of the MJO Modulation of Tropical Cyclogenesis Using an Empirical Index. J. Atmos. Sci., 66, 3061–3074.

Chang, Y. –L. and L. –Y. Oey, 2010: Eddy and wind forced heat transports in the Gulf of Mexico. J. Phys. Oceanogr., 40, 2727-2742.

Chang, Y-L., and L-Y. Oey, 2013: Coupled Response of the Trade Wind, SST Gradient, and SST in the Caribbean Sea, and the Potential Impact on Loop Current's Interannual Variability. Journal of Physical Oceanography, 43.7, 1325-1344.

Chen, M., P. Xie, J. E. Janowiak, and P. A. Arkin, 2002: Global Land Precipitation: A 50-yr Monthly Analysis Based on Gauge Observations, J. of Hydrometeorology, 3, 249-266.

Cook, K. H., and E. K. Vizy (2010), Hydrodynamics of the Caribbean lowlevel jet and its relationship to precipitation, J. Clim., 23, 1477–1494.

Collins, M., R. Knutti, J. Arblaster, J.–L. Dufresne, T. Fichefet, P. Friedlingstein, X. Gao, W.J. Gutowski, T. Johns, G. Krinner, M. Shongwe, C. Tebaldi, A.J. Weaver and M. Wehner, 2013: Long–term Climate Change: Projections, Com– mitments and Irreversibility. In: Climate Change 2013: The Physical Science Basis. Contribution of Working Group I to the Fifth Assessment Report of the Intergovernmental Panel on Climate Change [Stocker, T.F., D. Qin, G.–K. Plattner, M. Tignor, S.K. Allen, J. Boschung, A. Nauels, Y. Xia, V. Bex and P.M. Midgley (eds.)]. Cambridge University Press, Cambridge, United Kingdom and New York, NY, USA.

Crosbie, E., and Y. Serra, 2014: Intra-seasonal Modulation of Synoptic Scale Disturbances and Tropical Cyclone Genesis in the Eastern North Pacific. *J. Climate*, in press.

Dickinson, M. J., and coauthors, 1997: The March 1993 superstorm cyclongenesis: Incipient phase synoptic and convective scale flow interaction and model performance. Mon. Wea. Rev., 125, 3041-3072.

Dirmeyer, P. A., and J. L. KinterIII, 2009: The “Maya Express”: Floods in the U. S. Midwest. Eos Trans., AGU, 90(12) 101-108.

Domingues, R., G. Goni, F. Bringas, S.-K. Lee, H.-S. Kim, G. Halliwell, J. Dong, J. Morell and L. Pomales, 2015: Upper-ocean response to Hurricane Gonzalo (2014): salinity effects revealed by sustained and targeted observations from underwater gliders. Geophys. Res. Lett., Accepted.

Dominguez, F., P. Kumar, X.-Z. Liang, and M. Ting, 2006: Impact of Atmospheric Moisture Storage on Precipitation Recycling. Journal of Climate, 19, 1513–1530, doi:10.1175/JCLI3691.1.

Feng, S., Q. Hu, and R. J. Oglesby, Inuence of Atlantic sea surface temperatures on persistent drought in North America, Clim. Dyn., 37, 569{586, doi:10.1007/s00382-010-0835-x, 2011.

Ffield, A., 2007: Amazon and Orinoco River Plumes and NBC Rings: Bystanders or Participants in Hurricane Events? J. Climate, 20, 316–333. doi: http://dx.doi.org/10.1175/JCLI3985.1 .

Foltz, G.R. and M.J. McPhaden, 2009: Impact of barrier layer thickness on SST in the central tropical North Atlantic, J. Climate, **22**, 285–299.

Geil, K. L., Y. L. Serra, and X. Zeng, 2013: Assessment of CMIP5 model simulations of the North American monsoon system. J. Climate, 26, 8787–8801.

Giannini, A., Y. Kushnir, and M. A. Cane, 2000: Interannual variability of Caribbean rainfall, ENSO, and the Atlantic Ocean, J. Climate, 13, 297–311.

Graham, N. E., and T. P. Barnett, 1987: Sea surface temperature, surface wind divergence, and convection over tropical oceans. Science, 238, 657–659.

Granger, O. E., 1985: Caribbean climates, Prog. Phys. Geogr., 9, 16–43.

Haase-Schramm, A., Böhm, F., Eisenhauer, A., Dullo, W.-C., Joachimski, M.M., Hansen, B., Reitner, J., 2003. Sr/Ca ratios and oxygen isotopes from sclerosponges: temperature history of the Caribbean mixed layer and thermocline during the Little Ice Age. Paleoceanography 18, doi: 10.1029/2002PA0008

Hannah, W. M., and E. D. Maloney, 2014: The Moist Static Energy Budget in NCAR CAM5 Hindcasts during DYNAMO. J. Adv. Modeling Earth Sys., 6, doi:10.1002/2013MS000272.

Hartmann, D. L., and E. D. Maloney, 2001: The Madden-Julian oscillation, barotropic dynamics, and north Pacific tropical cyclone formation. Part II: Stochastic barotropic modeling. J. Atmos. Sci., 58, 2559-2570.

Hastenrath, S., 1976: Variations in low-latitude circulation and extreme climatic events in the tropical Americas, J. Atmos. Sci., 33, 202–215.

Hastenrath, S., 1978: On modes of tropical circulation and climatic anomaly, J. Atmos. Sci., 35, 2222–2231.

Herrera, E., V. Magana, and E. Caetano, 2014: Air-sea interactions and dynamical processes associated with the midsummer drought. Int. J. Climatology, doi:10.1002/joc.4077.

Hetzinger, S., Pfeiffer, M., Dullo, W.C., Garbe-Schonberg, D., Halfar, J., 2010. Rapid 20th century warming in the Caribbean and impact of remote forcing on climate in the northern tropical Atlantic as recorded in a Guadeloupe coral. Paleogeogr. Paleoclimatol. Paleoecol. 296, 111-124.

Higgins, R. W., W. Shi, 2001: Intercomparison of the Principal Modes of Interannual and Intraseasonal Variability of the North American Monsoon System. J. Climate, 14, 403–417.

Hirahara, S., M. Ishii, and Y. Fukuda, 2014: Centennial–Scale Sea Surface Temperature Analysis and Its Uncertainty. *J. Climate*, **27**, 57–75.

Hu, C. et al. 2004: The dispersal of the Amazon and Orinoco river water in the tropical Atlantic and Caribbean sea : Observation from space and S-PALACE floats, Deep-sea research II, 51.

Hu, Huancui and Francina Dominguez, 2015: Evaluation of Oceanic and Terrestrial sources of moisture for the North American Monsoon using Numerical Models and Precipitation Stable Isotopes. J. Hydrometeorology. In press.

Inoue, M., I. C. Handoh, and G. R. Bigg, 2002: Bimodal distribution of tropical cyclogenesis in the Caribbean: Characteristics and environmental factors. J. Climate, 15, 2897–2905.

Jayne, S. R. and J. Marotzke, 2002: The oceanic eddy heat transport. J. Phys. Oceaongraphy, 32, 3328-3345.

Jiang, X., and D. E. Waliser, 2009: Two dominant subseasonal variability modes of the eastern Pacific ITCZ, Geophys. Res. Lett., 36, L04704,

Jiang, X., M. Zhao, and D. E. Waliser, 2012: Modulation of tropical cyclone activity by the tropical intraseasonal oscillation over the Eastern Pacific in a high resolution GCM, Journal of Climate, 25, 6524-6538.

Jiang, X.-A., E. D. Maloney, J.-L. F. Li, and D. E. Waliser, 2013: Simulations of the eastern north Pacific intraseasonal variability in CMIP5 GCMs. J. Climate, 26, 3489-3510.

John, E. M., B. A Muhling, R. C. Perez, F. E. Muller-Karger, N. Melo, R. H. Smith, J. Lamkin, T. L. Gerard, and E. Malca, 2014: Amazon River water in the northeastern Caribbean Sea and its effect on larval reef fish assemblages during April 2009. Fish. Oceanogr., 23, 472-494.

Jouanno, J., J. Sheinbaum, B. Barnier, J.-M. Molines, and J. Candela, 2012: Seasonal and interannual modulation of the eddy kinetic energy in the Caribbean Sea. J. Phys. Oceanogr., 42, 2041–2055.

Jouanno, J. and J. Sheinbaum, 2013: Heat Balance and Eddies in the Caribbean Upwelling System . J. Phys. Oceanogr., 43, 1004-1014, DOI: 10.1175/JPO-D-12-0140.1 .

Kaplan, A., M. Cane, Y. Kushnir, A. Clement, M. Blumenthal, and B. Rajagopalan, 1998: Analyses of global sea surface temperature 1856–1991. *J. Geophys. Res.*, **103**, 18 567–18 589.

Kelly P and Mapes B (2011) Zonal mean wind, the Indian monsoon, and July drying in the western Atlantic subtropics. J. Geophys. Res. 116:D00Q07. doi:10.1029/2010JD015405.

Kilbourne, K.H., Quinn, T.M., Guilderson, T.P., Webb, R.S., Taylor, F.W., 2007. Decadal- to interannual-scale source water variations in the Caribbean Sea recorded by Puerto Rican coral radiocarbon. Climate Dynamics 29, 51-62.

Kim, D., A. H. Sobel, E. D. Maloney, D. M. W. Frierson, and I.-S. Kang, 2011: A systematic relationship between intraseasonal variability and mean state bias. J. Climate, 24, 5506-5520.

Kirtman, B. P., et al. (2014), The North American Multi-1 Model Ensemble (NMME): Phase-1 Seasonal to Interannual Prediction, Phase-2 Toward Developing Intra-Seasonal Prediction, Bull. Am. Meteorol. Soc., doi:10.1175/BAMS-D-12-00050.1

Kossin, J. P., and D. J. Vimont, 2007: A more general framework for understanding Atlantic hurricane variability and trends. Bull. Amer. Meteor. Soc., 88, 1767-1781.

Kozar, M. and V. Misra, 2012: Evaluation of twentieth-century Atlantic Warm Pool simulations in historical CMIP5 runs Clim. Dyn., 41(9-10), 2375-2391, doi:10.1007/s00382-012-1604-9.

Klotzbach, P. J., 2014: The Madden–Julian Oscillation's Impacts on Worldwide Tropical Cyclone Activity. J. Climate, 27, 2317–2330.

Knaff, J. A., 1997: Implications of summertime sea level pressure anomalies in the tropical Atlantic region, J. Climate, 10, 789–804.

Kushnir, Y., R. Seager, M. Ting, N. Naik, and J. Nakamura, Mechanisms of tropical Atlantic SST inuence on north american precipitation variability, Journal of Climate, 23, doi:10.1175/2010JCLI3172.1, 2010.

Lee, S.-K., D. B. Enfield, and C. Wang. What Drives Seasonal Onset and Decay of the Western Hemisphere Warm Pool? 2007: J. Clim., 20, 2133-2146

Lee, S.-K., C. Wang, and B.E. Mapes, 2009: A simple atmospheric model of the local and teleconnection responses to tropical heating anomalies. Journal of Climate, 22(2):227-284.

Lee, S.-K., D. B. Enfield and C. Wang, 2011: Future impact of differential inter-basin ocean warming on Atlantic hurricanes. J. Climate, 24, 1264-1275.

Lee S.-K., R. Atlas, D.B. Enfield, C. Wang and H. Liu, 2013a. Is There An Optimal ENSO Pattern That Enhances Large-scale Atmospheric Processes Conducive to Major Tornado Outbreaks in the U.S.? Journal of Climate, 26(5):1626-1642, doi:10.1175/JCLI-D-12-00128.1.

Lee, S.-K., C. R. Mechoso, C. Wang and J. D. Neelin, 2013b: Interhemispheric influence of the northern summer monsoons on the southern subtropical anticyclones. J. Climate, 26, 10193-10204. doi:http://dx.doi.org/10.1175/JCLI-D-13-00106.1.

Li, W., Li, L., Fu, R., Deng, Y., & Wang, H. (2011). Changes to the North Atlantic subtropical high and its role in the intensification of summer rainfall variability in the southeastern United States. Journal of Climate, 24(5), 1499-1506.

Liang, X.-Z., J. Zhu, K. E. Kunkel, M. Ting, and J. X. L. Wang, 2008: Do CGCMs simulate the North American monsoon precipitation seasonal–interannual variations? J. Climate, 21, 3755–3775.

Liu, H., C. Wang, S.-K. Lee, and D. B. Enfield, 2013: Atlantic warm pool variability in the CMIP5 simulations. Journal of Climate, 26: 5315-5336.

Liu, H.,C. Wang, S.-K. Lee, and D.B. Enfield, 2012: Atlantic warm pool variability in the IPCC-AR4 CGCM simulations. Journal of Climate, 25:5612-5628.

Liu, Y., S.-K. Lee, B. A. Muhling, J. T. Lamkin and D.B. Enfield, 2012: Significant reduction of the Loop Current in the 21st century and its impact on the Gulf of Mexico. J. Geophys. Res., 117, C05039, doi:10.1029/2011JC007555.

Liu, Y., S.-K. Lee, D. B. Enfield, B. A. Muhling, J. T. Lamkin, F. Muller-Karger and M. A. Roffer, 2015: Potential impact of climate change on the Intra-Americas Seas: Part-1. A dynamic downscaling of the CMIP5 model projections. J. Marine Syst., 148, 56-69, doi:10.1016/j.jmarsys.2015.01.007.

Magaña V., J. A. Amador and S. Medina, 1999: The midsummer drought over Mexico and Central America. J. Climate 12, 1577-1588.

Magaña, V., and Caetano, E., 2005: Temporal evolution of summer convective activity over the Americas warm pools. Geophys. Res. Lett., 32, doi:10.1029/2004GL021033.

Maloney, E. D., and D. L. Hartmann, 2000a: Modulation of hurricane activity in the Gulf of Mexico by the Madden-Julian oscillation. Science, 287, 2002-2004.

Maloney, E. D., and D. L. Hartmann, 2000b: Modulation of eastern north Pacific hurricanes by the Madden-Julian oscillation. J. Climate, 13, 1451-1460.

Maloney, E. D., and D. L. Hartmann, 2001: The Madden-Julian oscillation, barotropic dynamics, and north Pacific tropical cyclone formation. Part I: Observations. J. Atmos. Sci., 58, 2545-2558.

Maloney, E. D., and S. K. Esbensen, 2003: The amplification of east Pacific Madden-Julian oscillation convection and wind anomalies during June-November. J. Climate, 16, 3482-3497.

Maloney, E. D., X. Jiang, S.-P. Xie, and J. J. Benedict, 2014a: Process-oriented diagnosis of east Pacific warm pool intraseasonal variability. J. Climate, 27, 6305-6324.

Mapes, B. E., P. Liu, and N. Buenning, 2005: Indian monsoon onset and the Americas midsummer drought: Out-of equilibrium response to smooth seasonal forcing. J. Climate, 18, 1109–1115.

Martin, E.R., and C. Schumacher, 2011a,: Modulation of Caribbean precipitation by the Madden–Julian oscillation. J. Climate, 24, 813–824

Martin, E. R., and C. Schumacher, 2011b. The Caribbean low-level jet and its relationship with precipitation in IPCC AR4 models. J. Climate, 24, 5935–5950.

Martin, E. R., and C. Schumacher, 2012. The relationship between tropical warm pool precipitation, sea surface temperature, and large-scale vertical motion in IPCC AR4 models. J. Atmos. Sci. 69, 185–194.

Maupin, C.R., Quinn, T.M., 2008. Extracting a climate signal from the skeletal geochemistry of the Caribbean coral *Siderastrea siderea*. Geochemistry, Geophysics, Geosystems 9, 13.

Meehl, G. A., C. Covey, T. Delworth, M. Latif, B. McAvaney, J. F. B. Mitchell, R. J. Stouffer, and K. E. Taylor, 2007b: The WCRP CMIP3 multimodel dataset: A new era in climate change research. *Bull. Amer. Meteor. Soc.*, **88**, 1383–1394.

Mestas-Nuñez AM, Enfield DB, Zhang C (2007) Water vapor fluxes over the Intra Americas Sea: Seasonal and interannual variability and associations with rainfall. J Clim 20: 1910-1922.

Meinen, C.S., Baringer, M.O. & Garcia, R.F., 2010. Florida Current transport variability: An analysis of annual and longer-period signals. Deep Sea Research Part I: Oceanographic Research Papers, 57(7), pp.835–846.

Mignot., et al., Control of Salinity on the mixed layer depth in the world ocean. Part 2, Journal of Geophysical Research, 112, 2007.

Minder J. R., R. B. Smith, and A. D. Nugent, 2013: The Dynamics of Ascent-Forced Orographic Convection in the Tropics: Results from Dominica*. J. Atmos. Sci., 70, 4067–4088.

Misra, V., S. Chan, R. Wu, and E. Chassignet, 2009: Air-sea interaction over the Atlantic warm pool in the NCEP CFS. Geophys. Res. Lett., 36, L15702, doi:10.1029/2009GL038737.

Misra, V. , A. Stroman, and S. DiNapoli, 2013: The rendition of the Atlantic warm pool in the reanalyses Clim. Dyn., 41, 517-532, doi:10.1007/s00382-012-1474-1.

Misra, V. and S. DiNapoli, 2013: The observed teleconnection between the equatorial Amazon and the Intra-Americas Seas Clim. Dyn., 40(11-12), 2637-2649, doi:10.1007/s00382-012-1474-1.

Misra, V., H. Li, and M. Kozar, 2014: The precursors in the Intra-Americas Seas to seaseasonal climate variations over North America J. Geophys. Res. (Oceans), 119(5), 2938-2948, doi:10.1002/2014JC009911.

Misra, V. and H. Li, 2014: The seasonal climate predictability of the Atlantic Warm Pool and its Teleconnections Geophys. Res. Lett., 41(2), 661-666, doi:10.1002/2013GL058740.

Misra, V., H. Li, S. Brenner, B. Nag, and A. Mishra, 2015: The sensitivity of the regional coupled ocean-atmosphere downscaling of global reanalysis over the Intra-Americas Seas to the prescribed bathymetry. Ocean Modeling. Submitted.

Molinari, J., D. Knight, M. Dickinson, D. Vollaro, S. Skubis, 1997: Potential Vorticity, Easterly Waves, and Eastern Pacific Tropical Cyclogenesis. Mon. Wea. Rev., 125, 2699–2708.

Muñoz E., A. J. Busalacchi, S. Nigam and A. Ruiz-Barradas, 2008: Winter and summer structure of the Caribbean low-level jet. J. Climate, 21, 1260-1276.

Muñoz, E., and D. Enfield, 2011: The boreal spring variability of the Intra-Americas low-level jet and its relation with precipitation and tornadoes in the eastern United States. Climate Dyn., 36, 247–259, doi:10.1007/s00382-009-0688-3.

Neelin, J. D., M. Münnich, H. Su, J. E. Meyerson, and C. E. Holloway, 2006: Tropical drying trends in global warming models and observations. *Proc. Natl. Acad. Sci.* USA, **103**, 6110–6115.

Pailler, et al., The barrier layer in the western tropical Atlantic Ocean. Geophysical Research Letters, 26(14), 1999.

Patricola, C.M., R. Saravanan and P. Chang, 2014: The Impact of the El Nio-Southern Oscillation and Atlantic Meridional Mode on Seasonal Atlantic Tropical Cyclone Activity, J. Clim , 27 , 53115328. doi: http://dx.doi.org/10.1175/JCLI-D-13-00687.1.

Poveda, G., and Mesa, O. On the existence of Llor´o (the rainiest locality on Earth): Enhanced ocean-land-atmosphere interaction by a low-level jet. Geophys. Res. Lett. 27 (2000), 1675–1678.

Poveda G., and O. J. Mesa (1997), Feedbacks between hydrological processes in tropical South America and large-scale ocean-atmospheric phenomena, *J. Climate*, Vol. 10, No. 10, 2690-2702.

Poveda, G., and O. J. Mesa, 1999: The westerly Colombian low-level jet ("CHOCO") and two other low-level jets over Colombia: Climatology and variability during ENSO phases (In Spanish), Revista Academia Colombiana de Ciencias, Exactas, Físicas y Naturales, Vol. 23, No. 89, 517-528.

Poveda, G., et al. (2006), Annual and inter-annual variability of the present climate in northern South America and southern Mesoamerica, Palaeo-geogr. Palaeoclimatol. Palaeoecol., 234, 3–27.

Poveda, G., D. M. Álvarez, and O. A. Rueda (2011), Hydro-climatic variability over the Andes of Colombia associated with ENSO: a review of climatic processes and their impact on one of the Earth's most important biodiversity hotspots, *Climate Dynamics,* 36 (11-12), 2233-2249; DOI: 10.1007/s00382-010-0931-y.

Poveda, G., L. Jaramillo, and L. F. Vallejo, 2014: Seasonal precipitation patterns along pathways of South American low-level jets and aerial rivers, *Water Resour. Res*., 50, 98–118, doi:10.1002/2013WR014087.

Rauscher, S. A., F. Kucharski, and D. B. Enfield, 2011: The Role of Regional SST Warming Variations in the Drying of Meso–America in Future Climate Projections*. *J. Climate,* **24**, 2003–2016.

Rayner, N. A., D. E. Parker, E. B. Horton, C. K. Folland, L. V. Alexander, D. P. Rowell, E. C. Kent, and A. Kaplan, 2003: Global analyses of sea surface temperature, sea ice, and night marine air temperature since the late nineteenth century. *J. Geophys. Res.*, **108**, 4407.

Reynolds RW, Smith TM, Liu C, Chelton DB, Casey KS, Schlax MG (2007) Daily high-resolution blended analyses for sea surface temperature. J Clim 20:5473–5496.

Richter, I., and S.-P. Xie, 2008: On the origin of equatorial Atlantic biases in coupled general circulation models. Climate Dynamics, 31, 587-598.

Richter, I. and coauthors, 2014: Equatorial Atlantic variability and its relation to mean state biases in CMIP5. Clim. Dyn., 42, 171-188.

Richey, J.N., Poore, R.Z., Flower, B.P., Quinn, T.M., 2007. 1400 yr multiproxy record of clmiate variability from the northern Gulf of Mexico. Geology 2007, 4.

Richey, J.N., Poore, R.Z., Flower, B.P., Quinn, T.M., Hollander, D.J., 2009. Regionally coherent Little Ice Age cooling in the Atlantic Warm Pool. Geophysical Research Letters 36, 5.

Rosenheim, B.E., Swart, P.K., Thorrold, S.R., Eisenhauer, A., Willenz, P., 2005. Salinity change in the subtropical Atlantic: Secular increase and teleconnections to the North Atlantic Oscillation. Geophysical Research Letters 32.

Rousset, C. & Beal, L.M., 2014. Closing the transport budget of the Florida Straits. Geophysical research letters, 41(7), pp.2014GL059498–n/a.

Ruiz-Barradas, A. and S. Nigam, 2005: Warm season rainfall variability over the US great plains in observations, NCEP and ERA-40 Reanalyses, and NCAR and NASA Atmospheric Model Simulations, J. Climate, 18, 1808-1830.

Ruiz-Barradas, A. and S. Nigam, 2006: Great Plains hydroclimate variability: The view from North American Regional Reanalysis. J. Climate, 19, 3004-3010.

Rydbeck, A. V., E. D. Maloney, S.-P. Xie, J. Hafner, and J. Shaman, 2013: Remote forcing versus local feedback of east Pacific intraseasonal variability. J. Climate, 26, 3575–3596.

Rydbeck, A. V., and E. D. Maloney, 2014: Energetics of east Pacific easterly waves during intraseasonal events. J. Climate, 27, 7603-7621.

Schmitz, J. T., and S. L. Mullen, 1996: Water Vapor Transport Associated with the Summertime North American Monsoon as Depicted by ECMWF Analyses. Journal of Climate, 9, 1621–1634, doi:10.1175/1520-0442(1996)009<1621:WVTAWT>2.0.CO;2

Schubert, S., D. Gutzler, H. L. Wang, A. Dai, T. Delworth, C. Deser, K. Findell, R. Fu, W. Higgins, M. Hoerling, B. Kirtman, R. Koster, A. Kumar, D. Legler, D. Lettenmaier, B. Lyon, V. Magana, K. Mo, S. Nigam, P. Pegion, A. Phillips, R. Pulwarty, D. Rind, A. Ruiz–Barradas, J. Schemm, R. Seager, R. Stewart, M. Suarez, J. Syktus, M. F. Ting, C. Z. Wang, S. Weaver and N. Zeng, 2009: A US CLIVAR Project to Assess and Compare the Responses of Global Climate

Models to Drought–Related SST Forcing Patterns: Overview and Results. *J. Climate*, **22**(19): 5251–5272.

Smith, T. M., and R. W. Reynolds, T. C. Peterson, and J. Lawrimore, 2008: Improvements to NOAA's historical merged land–ocean surface temperature analysis (1880–2006). *J. Climate*, **21**, 2283–2296.

Schumann, S. A., J. Moser, G. A. Johnson, N. D. Walker, and S. A. Hsu, 1995: An overview of a strong winter low in the Gulf of Mexico 12-13 March 1993, National Weather Digest, 20 (1). Available from http://www.nwas.org/digest/papers/1995/Vol20-Issue1-Oct1995/Pg11-Schumann.pdf

Serra, Y. L., G. N. Kiladis, and M. F. Cronin, 2008: Horizontal and vertical structure of easterly waves in the Pacific ITCZ. J. Atmos. Sci., 65, 1266-1284.

Serra, Y. L., G. Kiladis, and K. Hodges, 2010: Tracking and Mean Structure of Easterly Waves Over the Intra-Americas Sea. J. Climate, 23, 4823-4840.

Serra, Y. L., X. Jiang, B. Tian, J. Amador Astua, E. D. Maloney, and G. N. Kiladis, 2014: Tropical intra-seasonal oscillations and synoptic variability. Annual Review of Environment and Resources, in press.

Sheffield, J., A. Barrett, B. Colle, R. Fu, K. L. Geil, Q. Hu, J. Kinter, S. Kumar, B. Langenbrunner, K. Lombardo, L. N. Long, E. Maloney, A. Mariotti, J. E. Meyerson, K. C. Mo, J. D. Neelin, Z. Pan, A. Ruiz-Barradas, Y. L. Serra, A. Seth, J. M. Thibeault, J. C. Stroeve, 2013: North American climate in CMIP5 experiments. Part I: Evaluation of 20th Century continental and regional climatology. J. Climate, 26, 9209-9245.

Sheinbaum, J. et al., 2002. Flow structure and transport in the Yucatan Channel. Geophysical research letters, 29(3), pp.10–11.

Skamarock, W. C., J. B. Klemp, J. Dudhia, D. O. Gill, D. M. Barker, M. G. Duda, X. Huang, W. Wang, and J. G. Powers, A description of the Advanced Research WRF Version 3, NCAR Technical Note, 2008.

Smith R. B., J. R. Minder, A. D. Nugent, T. Storelvmo, D. J. Kirshbaum, R. Warren, N. Lareau, P. Palany, A. James, and J. French, 2012: Orographic Precipitation in the Tropics: The Dominica Experiment. Bull. Amer. Meteor. Soc., 93, 1567–1579.

Smith, J.M., Quinn, T.M., Helmle, K.P., Halley, R.B., 2006. Reproducibility of geochemical and climatic signals in the Atlantic coral *Montastraea faveolata*. Paleoceanography 21, doi:10.1029/2005PA001187.

Sobel, A., Burleyson, C., and Yuter, S., 2011: Rain on small tropical islands. J. Geophys. Res., 116, D08102, doi:10.1029/2010JD014695.

Sprintall, J. and M. Tomczak, 1992:Evidence of the barrier layer in the surface layer of the tropics, Journal of Geophysical Research, 97 (C5), 7305–7316.

Taylor, K. E., R. J. Stouffer, and G. A. Meehl, 2012: An overview of CMIP5 and the experiment design. *Bull. Amer. Meteor. Soc.*, **93**, 485–498.

Ting, M., Y. Kushnir, R. Seager and L. Cuihua, 2011: Robust features of Atlantic multi-decadal variability and its climate impacts. *Geophys. Res. Lett.*, **38**, L17705.

Ting, M. F., Y. Kushnir, R. Seager and C. H. Li, 2009: Forced and Internal Twentieth–Century SST Trends in the North Atlantic. *J. Climate*, **22**(6): 1469–1481.

Toma, V. E., and P. J. Webster, 2010a: Oscillations of the intertropical convergence zone and the genesis of easterly waves. Part I: diagnostics and theory. Climate Dyn., 34, 587-604.

Toma, V. E., and P. J. Webster, 2010b: Oscillations of the Intertropical Convergence Zone and the genesis of easterly waves Part II: numerical verification. Climate Dyn., 34, 605-613.

Tuluy, H. A., G. M. Grandolini, E. J. Ijjasz-Vasquez, K. E. Kemper, and J. Zuleta, 2012: Project Appraisal Document on a Proposed Loan in the Amount of US$105,263,157.89 to the United Mexican States for the Modernization of the National Meteorological Service for Improved Climate Adaptation Project. World Bank, 1 pp.

Vimont, D. J., and J. P. Kossin, 2007: The Atlantic meridional mode and hurricane activity. Geophys. Res. Lett., 34, L07709, doi:10.1029/2007GL029683.

Vizy, E. and K. Cook, 2010: Influence of the Amazon/Orinoco Plume on the summertime Atlantic climate. Journal of Geophysical Research, 115 (D21), D21 112.

Wang, C., and D. B. Enfield, 2001: The tropical western hemisphere warm pool. Geophys. Res. Lett., 28, 1635-1638.

_____, and D. B. Enfield. A further study of the tropical Western Hemisphere Warm Pool. J. Climate, 6, 1476-1493 (2003).

_____, D. B. Enfield, S. –K. Lee, and C. Landsea. Influences of the Atlantic warm pool on Western Hemisphere summer rainfall and Atlantic hurricanes. J. Climate, 19, 3011-3028 (2006).

______, 2007: Variability of the Caribbean low-level jet and its relations to climate. Clim. Dyn., 29:411-422.

_____, and S. –K. Lee. Atlantic warm pool, Caribbean low-level jet, and their potential impact on Atlantic hurricanes. Geophys. Res. Lett., 34, (2007).

______, S. –K. Lee, and D. B. Enfield. Climate response to anomalously large and small Atlantic Warm pools during the summer. J. Climate, 21, 2437-2450 (2008a).

Wang, C., S.-K. Lee, and C. R. Mechoso, 2010: Interhemispheric influence of the Atlantic warm pool on the Southeastern Pacific. Journal of Climate, 23:404-418.

Wang, C., H. Liu, S.-K. Lee, and R. Atlas, 2011: Impact of the Atlantic warm pool on United States landfalling hurricanes. Geophysical Research Letters, 38, L19702, doi:10.1029/2011GL049265.

Wang, C., and L. Zhang, 2013: Multidecadal ocean temperature and salinity variability in the tropical North Atlantic: Linking with the AMO, AMOC and subtropical cell. Journal of Climate, 26, 6137-6162.

Wang, C., L. Zhang, S.-K. Lee., L. Wu, and C. R. Mechoso, 2014: A global perspective on CMIP5 climate model biases. Nature Climate Change , 4 , 201-205.

Wang, H., and R. Fu, 2002: Cross-equatorial flow and seasonal cycle of precipitation over South America. J. Clim., 15, 1591–1608.

Waylen, P. R., et al. (1996), Temporal and spatial variability of annual precipitation in Costa Rica and the Southern Oscillation, *Int. J. Climatol.*, 16, 173–193

Weisberg, R. H. On the evolution of SST over the PACS region, Abstracts of 76 'h AMS Annual Meeting, Atlanta, Georgia, Amer. Meteor. Soc., 378 (1996).

Xie, S.-P., 1996: Westward propagation of latitudinal asymmetry in a coupled ocean-atmosphere model. J. Atmos. Sci., 53, 3236–3250.

Xu, Z., P. Chang, I. Richter and W.-M. Kim, 2014: Diagnosing Southeast Tropical Atlantic SST and Ocean Circulation Biases in the CMIP5 Ensemble, Clim. Dyn. , DOI10.1007/s00382-014-2247-9.

Zhang, L., and C. Wang, 2012: Remote influences on freshwater flux variability in the Atlantic warm pool region. Geophysical Research Letters, 39, L19714, doi:10.1029/2012GL053530.

Zhang L., C. Wang and S.-K. Lee , 2014: Potential role of Atlantic warm pool-induced freshwater forcing in the Atlantic meridional overturning circulation: Ocean-sea ice coupled model simulations. Climate Dynam., doi:10.1007/s00382-013-2034-z., in-press .

Figure Captions

Figure 1: a) The climatological SST (in °C; from Extended Reynolds SST version 3 following Smith et al. 2008) for July-August-September-October (JASO) computed over 1950-2012 period. Similarly, composite JASO SST for the 10 b) largest and c) smallest AWP years between 1950-2012. The years of the composites in (b) and (c) are chosen from d) the time series of the JASO AWP area anomalies (in x 10^6 km^2). The bold black line in Figs. 1a-c indicate the 28.5°C isotherm.

Figure 2: Summertime (JJA) atmospheric teleconnections linked to large minus small AWP in (top panels) observations, (middle panel) AGCM and (bottom panels) simple model experiments (see Lee et al. 2009). Left panels show baroclinic steam function and rotational wind anomalies (750 minus 250hPa and divided by 2) and the right panels show barotropic streamfunction and rotational wind anomalies (750 plus 250mb divided by 2). The observations are based on ERSST3 and NCEP reanalysis, the AGCM results are from Wang et al. (2008), and the simple model results are from Lee et al. (2009). The unit for stream function is 10^{-6} m^2 s^{-1}.

Figure 3: The correlation of the June-October AWP area anomalies (SST from Reynolds et al. 2007) with corresponding a) rainfall anomalies (shaded; rainfall from Chen et al. 2002) and b) mean sea level pressure (MSLP) anomalies (shaded; MSLP from Saha et al. 2010) and regression of June-September AWP area anomalies on corresponding 925hPa wind anomalies (winds from Saha et al. 2010). The significant values at 95% confidence interval according to t-test are contoured and vectors are shown in red.

Figure 4: Linear trend in SST from "super ensemble" consisting of HadlSST1, KaplanSST2, ERSST3b and COBE2 reanalysis of the iCOADS data set. Masked (white) areas are where the sign of the trend in all 4 analysis products does not match; colored areas are average trends where all four products match in sign. Circles show sites where proxy reconstructions have positive (red) centennial trends or insignificant (white) trends. Magnitudes of proxy trends are generally higher than the observational data set. Boxes indicate areas for which Caribbean and Gulf of Mexico time series are calculated (see SM S.1).

Figure 5: The correlation of the June-July-August mean SST anomalies (OISST) with preceding December-February rainfall anomalies (CRU) over equatorial Amazon (outlined). These correlations are computed over 1995-2004 period after the linear trends in rainfall and SST are removed and only significant values at 90% confidence interval are shown. Adapted from Misra and DiNapoli (2013).

Figure 6: Climatological annual mean rainfall (mm/day) computed between 1998 and 2013 from TRMM 3B43 (0.25° resolution) and GPCP 1-degree daily (1DD) data (1° resolution) for four regions in the IAS: a) Caribbean wide (10-25°N, 60-90°W), b) Central America (8-22°N, 83-95°W), c) the Greater Antilles (16-24°N, 65-87°W), and d) the Lesser Antilles (11-20°N, 58-65°W).

Figure 7: Mean climatological SST (°C) in the Caribbean Sea for January-February-March (a) January-February-March, (b) April-May-June, (c) July-August-September, and (d) November-December-October from NOAA Ocean Watch blended SST product (http://oceanwatch.pfeg.noaa.gov/thredds/Satellite/aggregsatBA/ssta/catalog.html). The

mean is constructed over a period of 2003–2014.

Figure 8: The composite of Atlantic tropical cyclone track density (per 3°x3 °cell) for a) 10 largest AWP years (2010, 2005, 1998, 2012, 2011, 2006, 2003, 1987, 2004, 2008) and b) 10 smallest AWP years (1984,1986,1982,1985,1994,1992,1989,1993,1996,1991), selected between 1979-2012. There were 163 and 90 named tropical cyclones in the 10 selected largest and smallest AWP years respectively.

Figure 9. Incidents of intense (F3–F5) U.S. tornadoes in April-May for (a) the top 10 most active years, (b) 10 least active years during 1950–2010 obtained from Severe Weather database. Green indicates F3, blue F4, and red F5 tornadoes. Anomalous moisture transport for the (c) 10 most active and (d) 10 least active U.S. tornado years in April-May during 1950–2010 obtained from NCEP reanalysis. The unit for moisture transport is kg $m^{-1}s^{-1}$. The small boxes in (c) and (d) indicate the central and eastern U.S. region frequently affected by intense tornadoes (30–40N, 100–80W). This figure is reproduced from Lee et al. (2013).

Figure 10: The average monthly Atlantic Warm pool areas (in $x10^6$ km^2) from 1909–2005 based on various CMIP5 20th century simulations and ERSSTv3 observations. Each cell in the table is color coded (cool colors indicate a small AWP; warm colors indicate a large AWP) in order to show the average seasonal evolution of the Atlantic Warm Pool's areal extent. Adapted from Kozar and Misra (2012).

Figure 11: Annual mean SST biases in CMIP5 (a) and CMIP3 (b) model ensembles. The biases are referenced to observed Reynolds SST. After Xu et al. 2014.

Fig. 12: Anomaly correlation (AC) skill of SST prediction for seasonal means of June-July-August (JJA). AC is computed based on the NMME hindcasts over the 1981-2010 period. The NMME ensemble initialized in March was used.

Figure 13: Same as Fig. 13 but for seasonal mean June-July-August (JJA) precipitation anomaly.

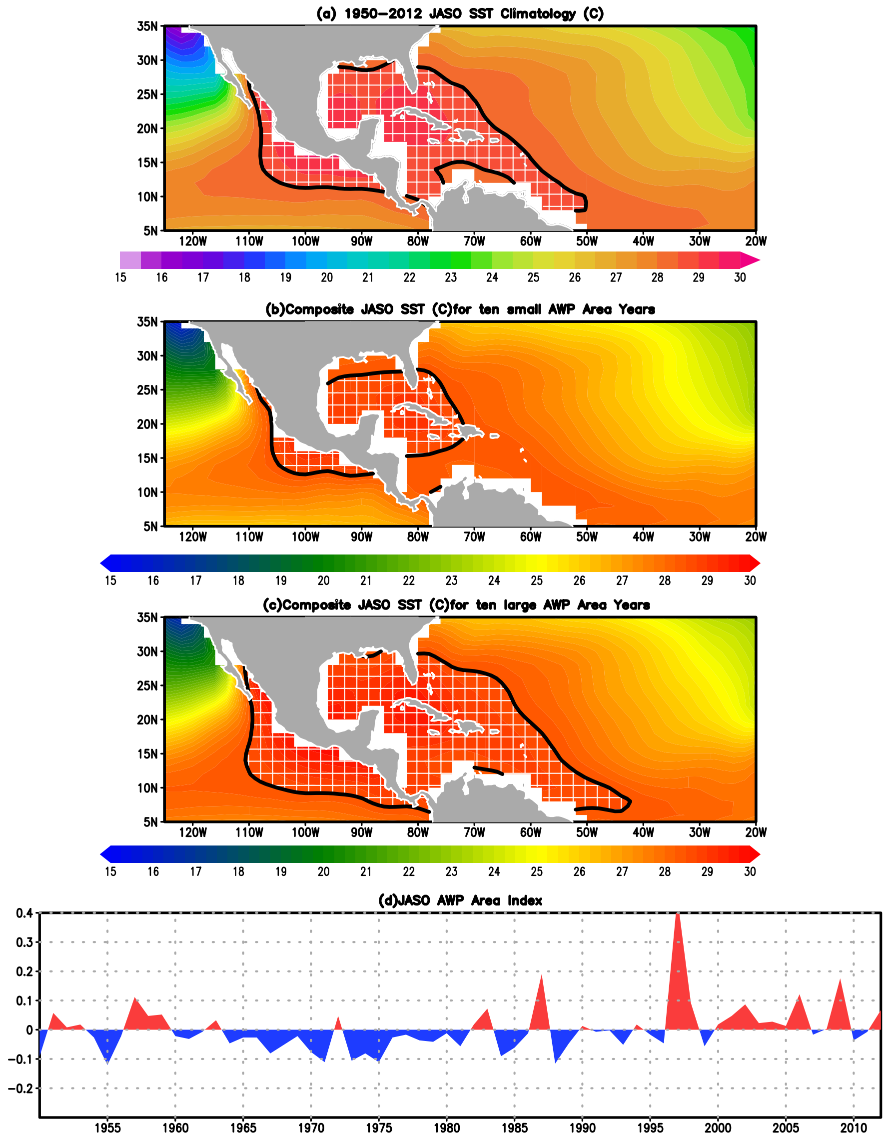

Figure 1: a) The climatological SST (in °C; from Extended Reynolds SST version 3 following Smith et al. 2008) for July-August-September-October (JASO) computed over 1950-2012 period. Similarly, composite JASO SST for the 10 b) largest and c) smallest AWP years between 1950-2012. The years of the composites in (b) and (c) are chosen from d) the time series of the JASO AWP area anomalies (in x 10^6 km^2). The bold black line in Figs. 1a-c indicate the 28.5°C isotherm.

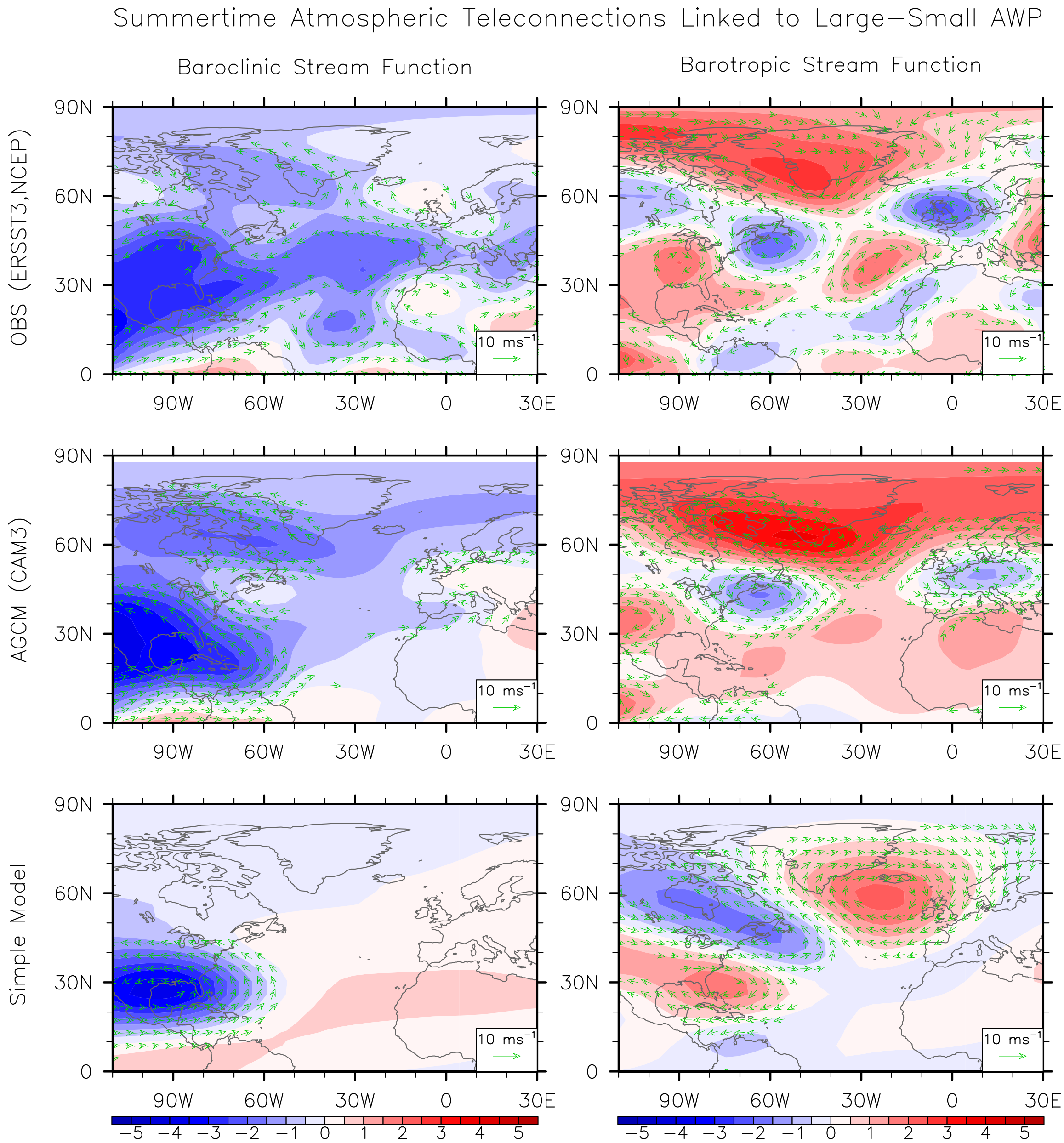

Figure 2: Summertime (JJA) atmospheric teleconnections linked to large minus small AWP in (top panels) observations, (middle panel) AGCM and (bottom panels) simple model experiments (see Lee et al. 2009). Left panels show baroclinic steam function and rotational wind anomalies (750 minus 250hPa and divided by 2) and the right panels show barotropic streamfunction and rotational wind anomalies (750 plus 250mb divided by 2). The observations are based on ERSST3 and NCEP reanalysis, the AGCM results are from Wang et al. (2008), and the simple model results are from Lee et al. (2009). The unit for stream function is 10^{-6} m^2 s^{-1}.

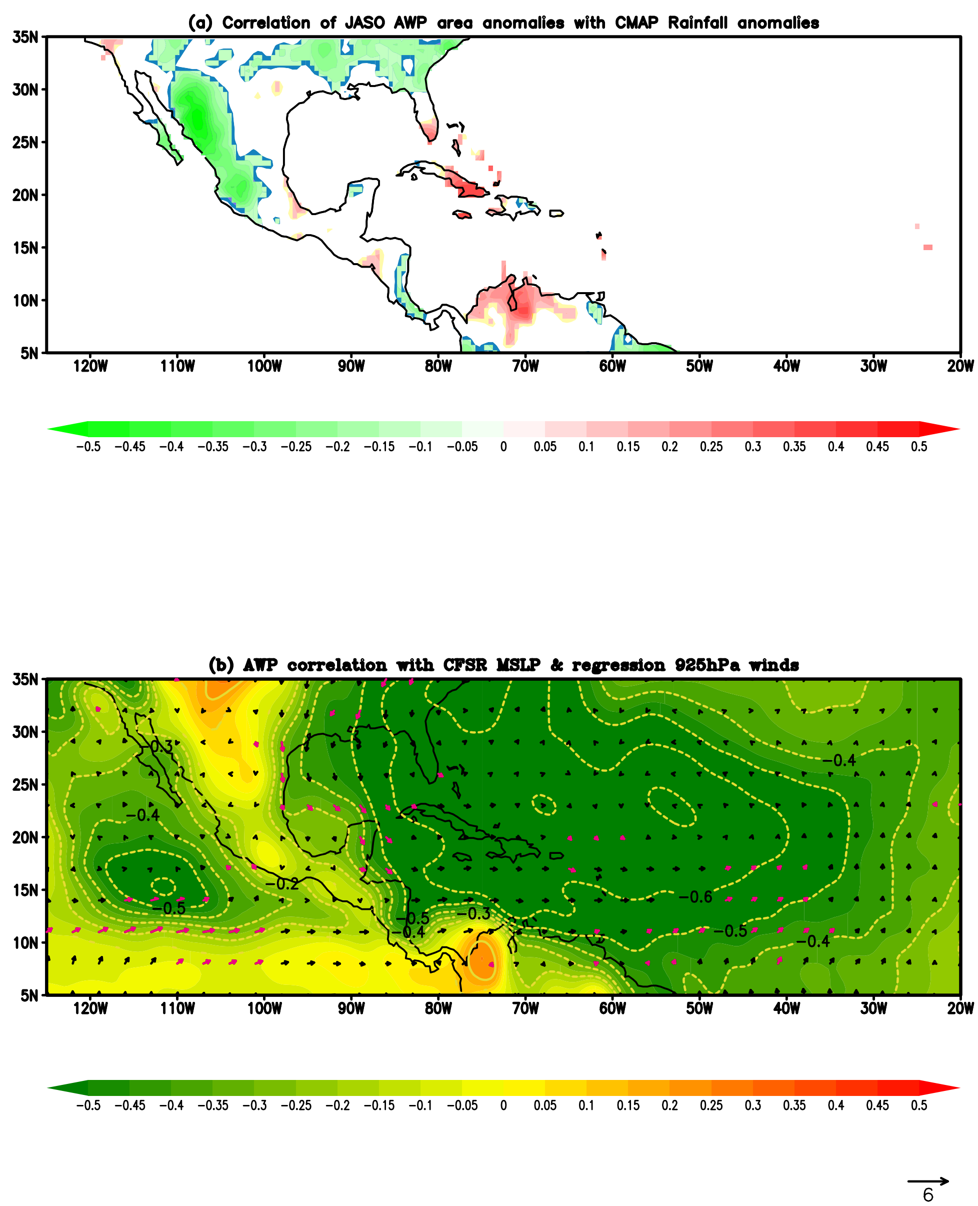

Figure 3: The correlation of the June-October AWP area anomalies (SST from Reynolds et al. 2007) with corresponding a) rainfall anomalies (shaded; rainfall from Chen et al. 2002) and b) mean sea level pressure (MSLP) anomalies (shaded; MSLP from Saha et al. 2010) and regression of June-September AWP area anomalies on corresponding 925hPa wind anomalies (winds from Saha et al. 2010). The significant values at 95% confidence interval according to t-test are contoured and vectors are shown in red.

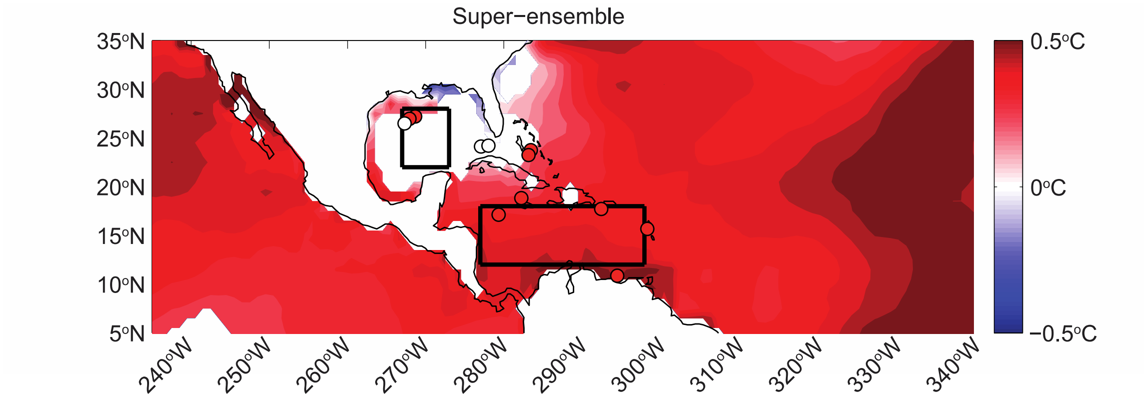

Figure 4: Linear trend in SST from "super ensemble" consisting of HadlSST1, KaplanSST2, ERSST3b and COBE2 reanalysis of the iCOADS data set. Masked (white) areas are where the sign of the trend in all 4 analysis products does not match; colored areas are average trends where all four products match in sign. Circles show sites where proxy reconstructions have positive (red) centennial trends or insignificant (white) trends. Magnitudes of proxy trends are generally higher than the observational data set. Boxes indicate areas for which Caribbean and Gulf of Mexico time series are calculated (see SM S.1).

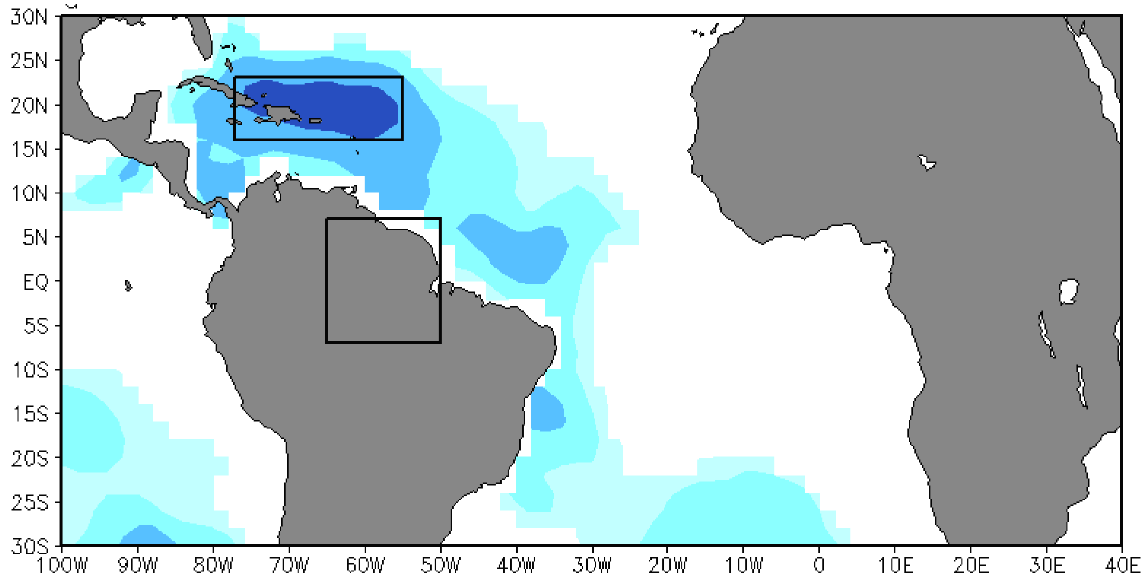

Figure 5: The correlation of the June-July-August mean SST anomalies (OISST) with preceding December-February rainfall anomalies (CRU) over equatorial Amazon (outlined). These correlations are computed over 1995-2004 period after the linear trends in rainfall and SST are removed and only significant values at 90% confidence interval are shown. Adapted from Misra and DiNapoli (2013).

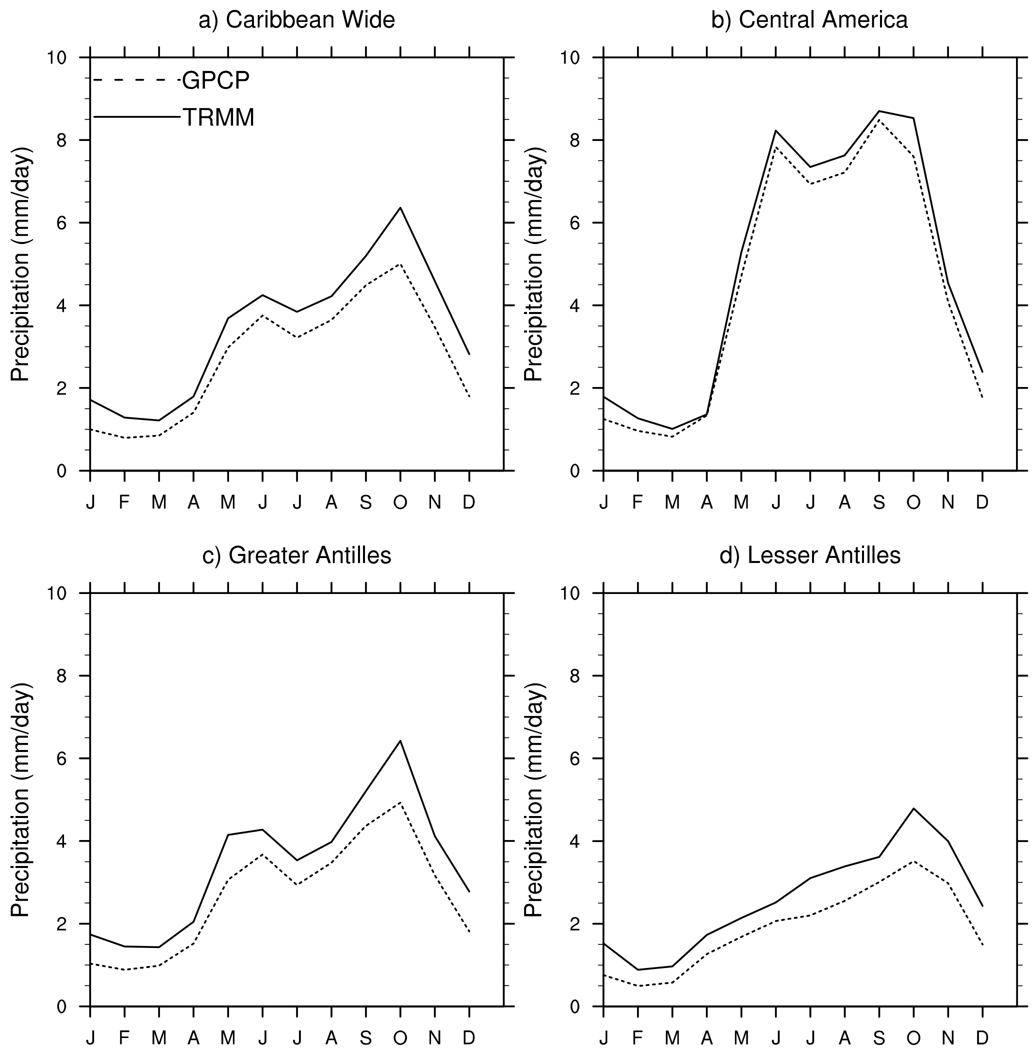

Figure 6: Climatological annual mean rainfall (mm/day) computed between 1998 and 2013 from TRMM 3B43 (0.25° resolution) and GPCP 1-degree daily (1DD) data (1° resolution) for four regions in the IAS: a) Caribbean wide (10-25°N, 60-90°W), b) Central America (8-22°N, 83-95°W), c) the Greater Antilles (16-24°N, 65-87°W), and d) the Lesser Antilles (11-20°N, 58-65°W).

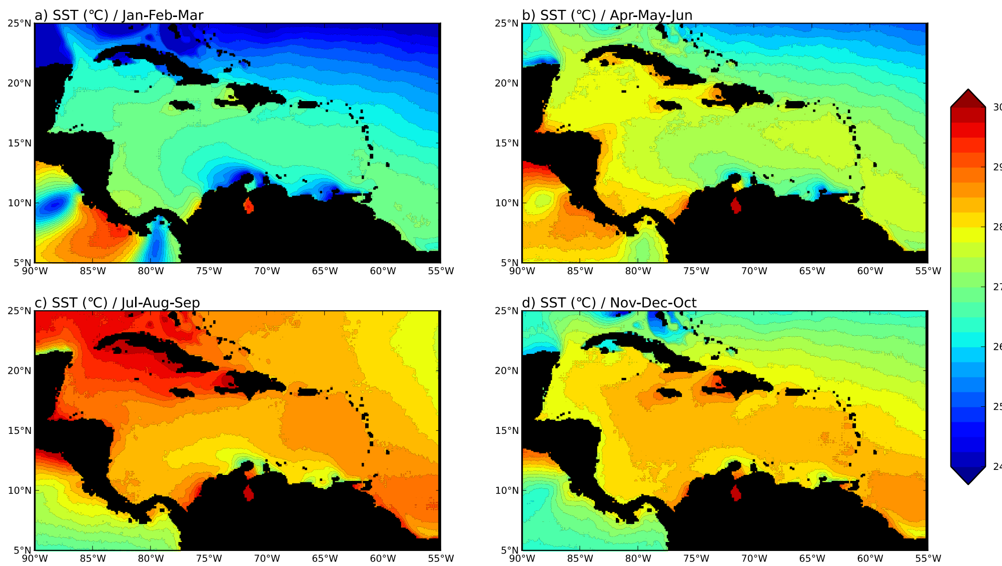

Figure 7: Mean climatological SST (°C) in the Caribbean Sea for January-February-March (a) January-February-March, (b) April-May-June, (c) July-August-September, and (d) November-December-October from NOAA Ocean Watch blended SST product (http://oceanwatch.pfeg.noaa.gov/thredds/Satellite/aggregsatBA/ssta/catalog.html). The mean is constructed over a period of 2003–2014.

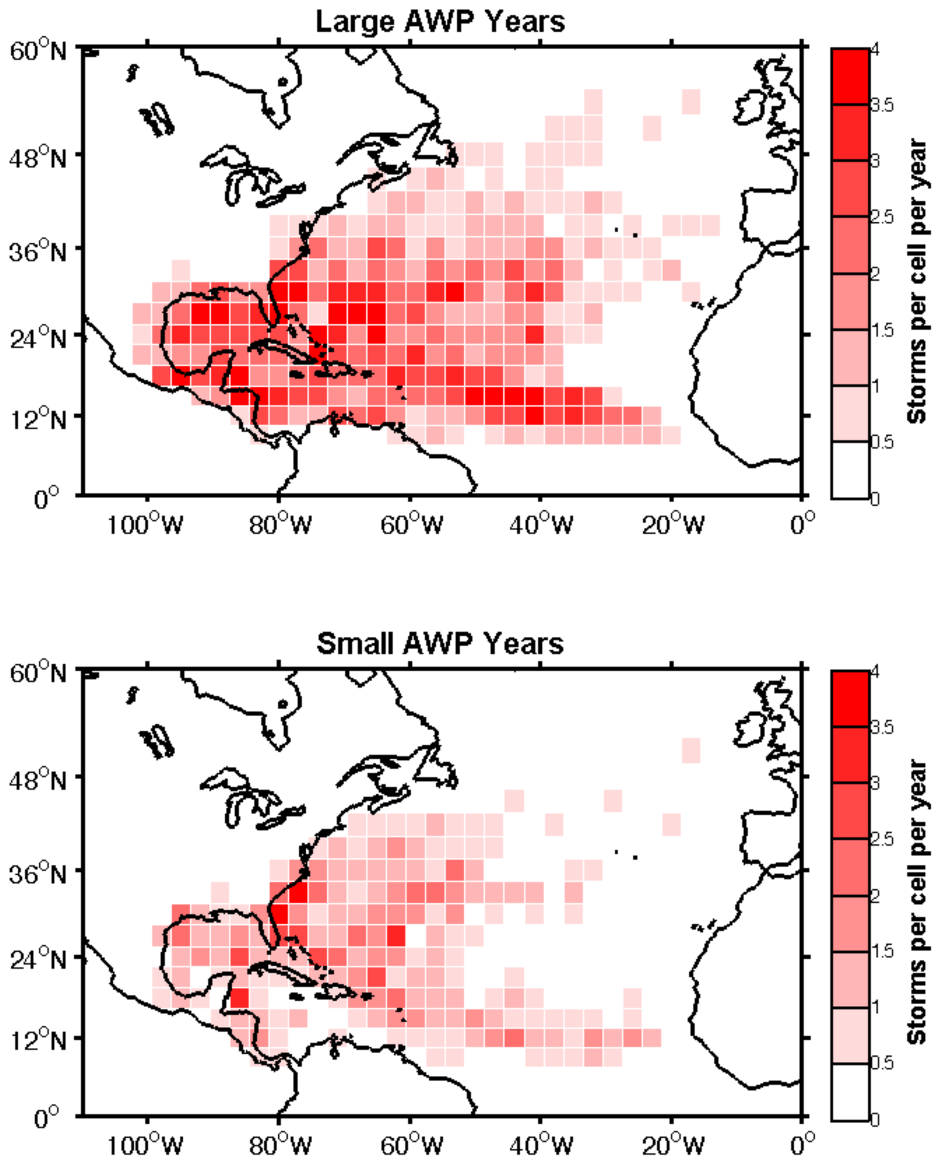

Figure 8: The composite of Atlantic tropical cyclone track density (per 3°x3 °cell) for a) 10 largest AWP years (2010, 2005, 1998, 2012, 2011, 2006, 2003, 1987, 2004, 2008) and b) 10 smallest AWP years (1984,1986,1982,1985,1994,1992,1989,1993,1996,1991), selected between 1979-2012. There were 163 and 90 named tropical cyclones in the 10 selected largest and smallest AWP years respectively.

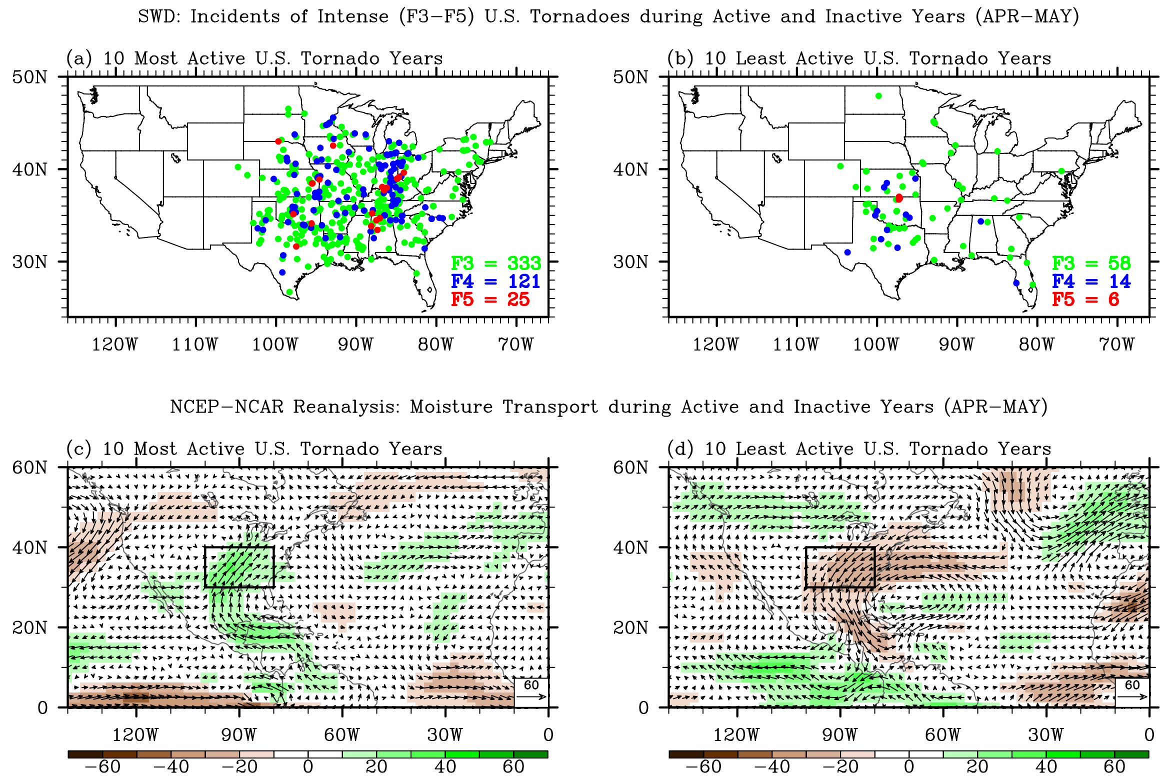

Figure 9. Incidents of intense (F3–F5) U.S. tornadoes in April-May for (a) the top 10 most active years, (b) 10 least active years during 1950–2010 obtained from Severe Weather database. Green indicates F3, blue F4, and red F5 tornadoes. Anomalous moisture transport for the (c) 10 most active and (d) 10 least active U.S. tornado years in April-May during 1950–2010 obtained from NCEP reanalysis. The unit for moisture transport is kg $m^{-1}s^{-1}$. The small boxes in (c) and (d) indicate the central and eastern U.S. region frequently affected by intense tornadoes (30–40N, 100–80W). This figure is reproduced from Lee et al. (2013).

Seasonal Cycle of AWP Area

Months	Jan	Feb	Mar	Apr	May	Jun	Jul	Aug	Sep	Oct	Nov	Dec
ERSST v3	0.00	0.00	0.00	0.01	0.05	0.40	2.49	3.71	3.99	1.63	0.07	0.00
BCC-CSM1-1	0.00	0.00	0.00	0.00	0.00	0.01	0.29	0.68	0.38	0.02	0.00	0.00
CanESM2	0.00	0.00	0.00	0.01	0.00	0.03	0.29	0.83	0.78	0.15	0.01	0.00
CCSM4	0.00	0.00	0.00	0.02	0.02	0.04	0.51	1.31	1.12	0.12	0.00	0.00
CNRM-CM5	0.00	0.00	0.00	0.01	0.02	0.07	0.27	0.79	0.85	0.28	0.03	0.01
CSIRO-Mk3.6	0.00	0.00	0.00	0.00	0.04	0.43	2.06	2.99	3.09	1.42	0.26	0.00
GFDL-CM3	0.00	0.00	0.00	0.00	0.00	0.06	0.54	1.18	0.76	0.11	0.00	0.00
GFDL-ESM2G	0.00	0.00	0.00	0.00	0.00	0.01	0.18	0.81	0.81	0.22	0.01	0.00
GFDL-ESM2M	0.00	0.00	0.00	0.00	0.00	0.01	0.14	0.70	0.64	0.26	0.02	0.00
GISS-E2-H	0.00	0.00	0.02	0.09	0.19	0.26	0.31	0.70	1.02	0.90	0.24	0.01
GISS-E2-R	0.00	0.00	0.02	0.16	0.40	0.68	1.73	3.55	3.83	2.85	1.04	0.09
HadGEM2-ES	0.05	0.04	0.06	0.10	0.21	0.33	0.57	1.37	1.48	0.57	0.21	0.10
INM-CM4	0.01	0.00	0.00	0.01	0.02	0.00	0.01	0.06	0.02	0.00	0.00	0.01
IPSL-CM5A-LR	0.00	0.00	0.00	0.00	0.00	0.03	0.07	0.21	0.07	0.01	0.00	0.00
MIROC5	0.00	0.00	0.00	0.02	0.04	0.09	0.11	0.23	0.26	0.12	0.02	0.00
MPI-ESM-LR	0.00	0.00	0.00	0.00	0.00	0.08	0.71	2.05	2.45	1.01	0.14	0.01
MRI-CGCM3	0.00	0.00	0.00	0.00	0.00	0.02	0.12	0.39	0.38	0.18	0.01	0.00
NorESM1-M	0.00	0.00	0.00	0.00	0.00	0.00	0.00	0.03	0.02	0.00	0.00	0.00

0.00	0.05	0.10	0.15	0.20	0.30	0.40	0.60	0.80	1.00	1.25	1.50	1.75	2.00	2.50	3.00	3.50	4.00

AREA OF 28.5°C MONTHLY AVERAGED ISOTHERM (10^6 km^2)

Figure 10: The average monthly Atlantic Warm pool areas (in x10^6 km^2) from 1909–2005 based on various CMIP5 20th century simulations and ERSSTv3 observations. Each cell in the table is color coded (cool colors indicate a small AWP; warm colors indicate a large AWP) in order to show the average seasonal evolution of the Atlantic Warm Pool's areal extent. Adapted from Kozar and Misra (2012).

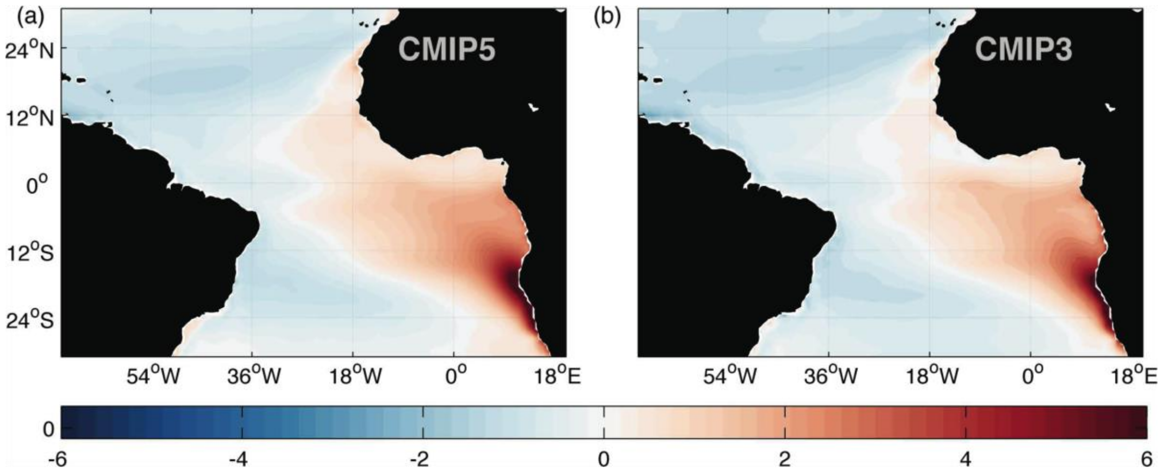

Figure 11: Annual mean SST biases in CMIP5 (a) and CMIP3 (b) model ensembles. The biases are referenced to observed Reynolds SST. After Xu et al. 2014.

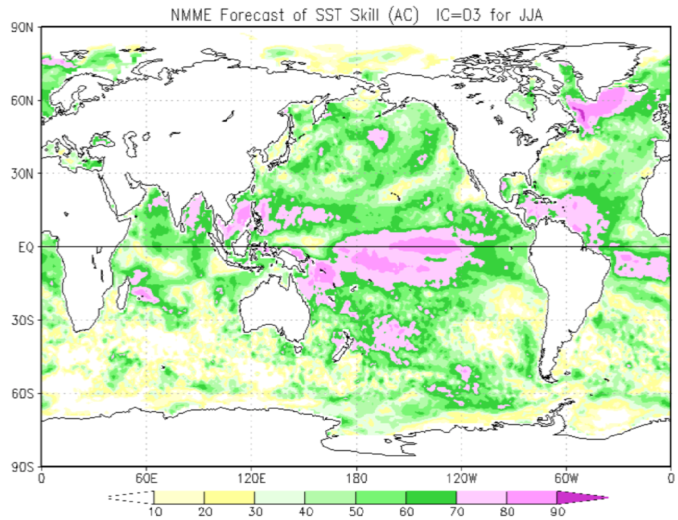

Fig. 12: Anomaly correlation (AC) skill of SST prediction for seasonal means of June-July-August (JJA). AC is computed based on the NMME hindcasts over the 1981-2010 period. The NMME ensemble initialized in March was used.

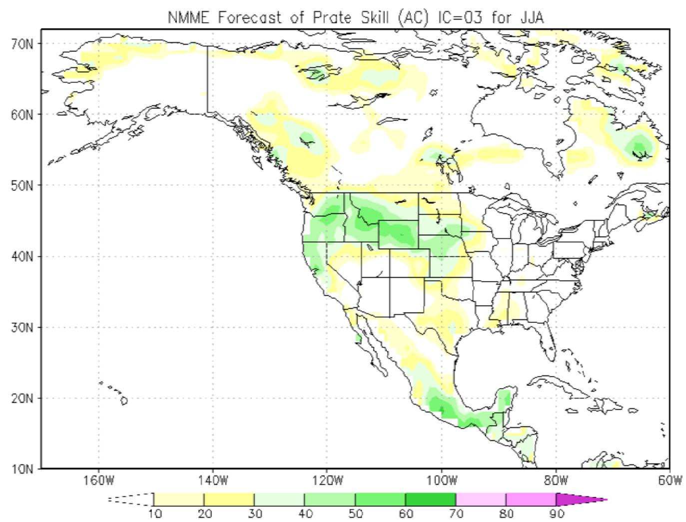

Figure 13: Same as Fig. 12 but for seasonal mean June-July-August (JJA) precipitation anomaly.

Supplemental Material

Click here to download Supplemental Material: bams-supplementary-R.docx